TRIUMF

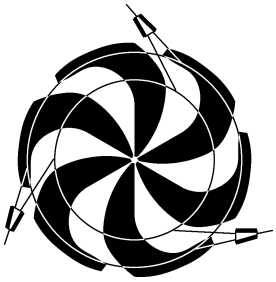

ANNUAL REPORT
SCIENTIFIC ACTIVITIES
2004

ISSN 1492-417X

CANADA'S NATIONAL LABORATORY FOR PARTICLE AND NUCLEAR PHYSICS

OPERATED AS A JOINT VENTURE

MEMBERS:

THE UNIVERSITY OF ALBERTA
THE UNIVERSITY OF BRITISH COLUMBIA
CARLETON UNIVERSITY
SIMON FRASER UNIVERSITY
THE UNIVERSITY OF TORONTO
THE UNIVERSITY OF VICTORIA

ASSOCIATE MEMBERS:

THE UNIVERSITY OF GUELPH
THE UNIVERSITY OF MANITOBA
McMASTER UNIVERSITY
L'UNIVERSITÉ DE MONTRÉAL
QUEEN'S UNIVERSITY
THE UNIVERSITY OF REGINA
SAINT MARY'S UNIVERSITY

UNDER A CONTRIBUTION FROM THE
NATIONAL RESEARCH COUNCIL OF CANADA

OCTOBER 2005

The contributions on individual experiments in this report are outlines intended to demonstrate the extent of scientific activity at TRIUMF during the past year. The outlines are not publications and often contain preliminary results not intended, or not yet ready, for publication. Material from these reports should not be reproduced or quoted without permission from the authors.

ISAC DIVISION

INTRODUCTION

The following ISAC sections describe the various activities in ISAC-I operation, ISAC-I developments and the progress in ISAC-II during 2004. Although there have been many highlights during the year, only a few are outlined here. The availability of the first target station to be commissioned (ITW) was remarkably near 90%, whereas the newer target station (ITE) was only 50%, reflecting the fact that ITE was used extensively for developing high power targets and an ECR ion source. Nine different targets were installed during the year (four Ta, three SiC, one $CaZrO_3$ and one ZrC). Several were compromised as a result of damage caused by the proton beam. The on-line testing of the ECR ion source has shown that the design must be modified to provide better ionization efficiencies in the high gas environment from the target. The charge state booster was used to examine the charge distribution of various species. A resonant laser ion source was used to provide a beam of ^{62}Ga from a SiC target. Development work during the year focused on developing schemes to provide laser-ionized beams of Al and Ga. In ISAC-II, all of the medium beta superconducting rf cavities have been fabricated, chemically treated and are now at TRIUMF. Two cryomodule tanks have been delivered to TRIUMF. Most of the liquid helium plant has been delivered to ISAC, is being installed, and commissioning will begin early in 2005. Good progress is being made on achieving adequate cavity tuning and rf coupling. Components required for the S-bend HEBT connecting the ISAC-I DTL to the ISAC-II medium beta accelerator are ready for installation during the 2005 winter shutdown. The ISAC-II installation schedule predicts that the medium beta section should be completed in time to accelerate a beam from the DTL through five cryomodules by the end of 2005.

ISAC OPERATIONS

This year, routine RIB operation provided beams to DRAGON and TUDA in the high energy area and to low energy experiments at LTNO, 8π, GPS1-3, BNMR and Osaka. As in previous years, the first quarter was devoted to shutdown activities. Beam schedule 105 began in the second quarter and carried on through the summer. Beam schedule 106 followed a short shutdown in September. An overview of RIB operation is shown in Fig. 206 in terms of the weekly proton beam exposure of the production targets. The total proton exposure is given for each target. The hours of RIB and stable beam operation for schedules 105 and 106 are shown in Figs. 207–210.

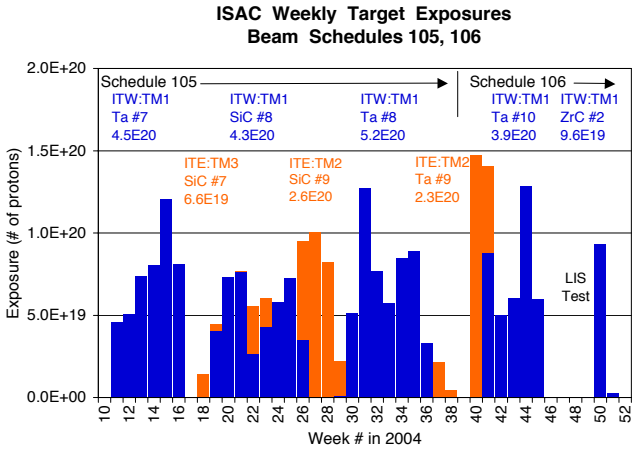

Fig. 206. Integral target exposures by week for RIB delivery in 2004.

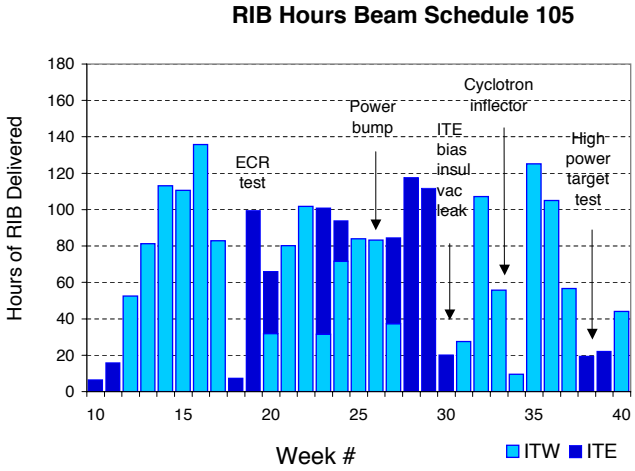

Fig. 207. Weekly hours of RIB beam available to experiments during schedule 105.

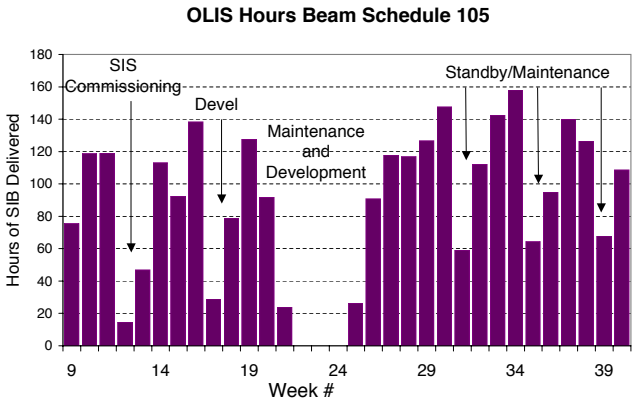

Fig. 208. Weekly hours of stable beam available to experiments during schedule 105.

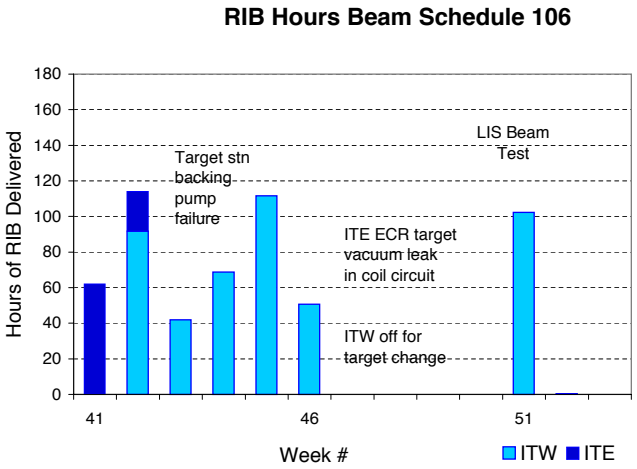

Fig. 209. Weekly hours of RIB beam available to experiments during schedule 106.

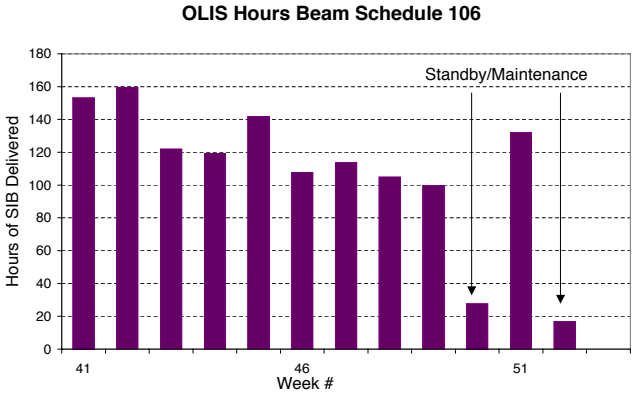

Fig. 210. Weekly hours of stable beam available to experiments during schedule 106.

Operational performance statistics are provided for the ISAC beam production of RIB from ITW and ITE and stable beam from OLIS. These are summarized separately for each beam schedule in Tables XXIX–XL. The summary performance statistics are given in Table XLI. Here it can be seen that 89.2% availability for ITW reflects its nature as a fully commissioned target station, whereas the 50.6% availability for ITE operation reflects the reality of the challenges of commissioning the ECR and high power targets. This summary information includes the effects of experiment operational performance, ISAC system performance and the availability of proton beam from the cyclotron and also includes overhead as well as downtime components. Some interpretation is required to extract the relevance of beam time in the context of operational constraints not accounted for during beam scheduling. This year, several targets were damaged during operation resulting in lower yields and consequently RIB rates to users much less than expected when the beam time was scheduled. There is no easy way to represent this in the performance statistics, other than to acknowledge the fact that yields were low and there was evidence of target damage. The target damage likely occurred due to a mismatch between the delivered power density of the proton beam compared to that estimated for setting the target operating parameters, the most critical being the central temperature. Efforts are under way to understand and remedy these problems. On the other hand, the ISAC systems were for the most part very reliable. There were only a few notable exceptions. Power outages in week #26 that affected cyclotron availability, a vacuum leak in a HV insulator damaged by sparking that was caused by a water leak in the HV enclosure on top of the east target station in week #30, and finally, a vacuum leak from a coil cooling circuit on TM3 caused the cancellation of ECR operation in November.

A major milestone was achieved in the last weeks of beam schedule 106 when the first RIB operation with a laser ion source was demonstrated.

The summary of beam to experiments for the year is given in Table XLII, and the summary of the isotopic beam delivery is given in Table XLIII.

Two new operators, who had been recruited in October, 2003, completed their training and assumed shift responsibilities in May, 2004, bringing the complement of shift operators to six which is still inadequate to properly serve the needs of a challenging science program at a multiple source RIB facility. The sixth operator provided support for afternoon activities Monday to Friday and filled in for operator absences.

Several new Web based applications were introduced, including a new e-log, NCR (non-conformance report) and revised electronic work permit system. A number of operator environment tools were developed including: improved tuning and save routines, segregated strategic alarm handling, electrostatic steering optimization program, IBRMS bridge display, and firewall protection of the ISAC Operations network. Applications and assistance were also provided for the TRILIS and SCRF projects. The ISAC-II control room was equipped with one off-line work station which was used for development purposes.

Documentation and training responsibilities continue to command the full-time attention of the ISAC Operations Documentation and Training Coordinator. After the training of the new operators was completed in April, work resumed on the design phase of the SAT program, which was completed and approved. The development phase will carry over into 2005. Learning objectives were established for all of the previously recorded training videos; an important aspect of the evaluation phase of SAT.

The members of the ISAC Operations group take great pride in their contributions to the successes of the experiments and major ISAC milestones that have

been highlighted elsewhere in this Annual Report. In the coming year, in addition to providing beam for the scheduled experiments and performing systems maintenance, the major effort will be to complete the SAT training program for ISAC operators, migrate many of the control functions to the ISAC-II Control Room, and continue to improve the ability of ISAC Operations to provide the beams of interest to the ISAC science program.

Table XXIX. ITW beam schedule 105 (surface ion source targets used: Ta #7/8/10 and SiC #8): February 23 – October 4 (weeks 9–40). ITW beam to ISAC experiments (hours).

Expt	Line	Sched	Actual	Tune	Off	Total
Yield	ILY	426	64.4	2.8	0.0	67.2
ICS	ICS	0	1.7	0.0	0.0	1.7
E816	β-NMR	156	0.0	0.0	0.0	0.0
E817	β-NMR	348	270.6	15.4	16.2	302.2
E824	DRAGON	78	22.4	2.9	2.6	27.9
E871	Osaka	192	191.8	0.9	9.8	202.5
E903	Osaka	264	119.6	10.4	0.0	130.0
E909	8π	95	76.3	1.9	6.3	84.5
E920	Polarizer	120	41.7	0.0	0.3	42.0
E921	8π	156	138.7	0.4	19.8	158.9
E973	8π	276	170.0	1.0	6.5	177.5
E984	8π	96	67.9	7.2	3.4	78.5
E989	DRAGON	288	173.0	5.4	1.9	180.3
E991	GPS3	156	81.2	2.3	3.5	87.0
LIS	IMS	180	44.1	0.0	0.0	44.1
Subtotals		2831	1463.4	50.6	70.3	1584.3
Available					44.0	44.0
Totals		2831	1463.4	50.6	114.3	1628.3

Total RIB experiment time = 1628.3 hours
Combined facility efficiency = 92.9%

Table XXX. ITW beam schedule 105: ITW systems downtime and overhead.

ISAC systems	Hours
Downtime – unscheduled	
Beam lines	1.3
Controls	30.2
Elec P/S	5.1
Mag P/S	0.5
RF controls	2.0
Ion source	45.8
Polarizer	21.9
Safety	0.2
Site power	17.4
Subtotal	124.4
Downtime – scheduled (overhead)	
Cyclotron maintenance	255.8
Cyclotron development	83.4
Beam line 2A off	389.0
ISAC shutdown	168.0
ISAC idle	347.8
Procedures	510.3
Target conditioning	435.5
Target change	1375.9
ITW startup	24.9
ITW cooldown	31.5
Q-exch stripper	0.2
Subtotal	3622.3
Total	3746.7

Table XXXI. ITE beam schedule 105: ITE beam to ISAC experiments (hours).

Expt	Sched	Actual	Tune	Off	Total
Yield	444	57.9	1.3	0.3	59.5
ICS	0	6.5	0.0	0.0	6.5
E816	144	178.7	6.8	2.0	187.5
E824	120	57.6	5.7	0.0	63.3
E984	0	0.0	0.0	0.0	0.0
E985	168	189.4	2.6	13.8	205.8
E989	96	7.8	2.7	0.8	11.3
E991	36	0.0	0.0	0.0	0.0
E995	0	15.4	0.0	0.5	15.9
Totals	1008	513.3	19.1	17.4	549.8

Total RIB experiment time = 593.2 hours
Combined facility efficiency = 74.1%

Table XXXII. ITE beam schedule 105: ITE systems downtime and overhead.

ISAC systems	Hours
Downtime – unscheduled	
Beam lines	4.0
Controls	10.2
Elec P/S	65.6
Ion source	108.3
Pre-buncher	3.6
DTL rf	0.3
Services	4.5
Site power	0.5
Vacuum	9.9
Subtotal	206.9
Downtime – scheduled (overhead)	
Cyclotron maintenance	86.9
Cyclotron development	36.0
Beam line 2A off	49.5
ISAC development	175.4
ISAC idle	1133.5
ISAC maintenance	20.3
Procedures	273.9
Shutdown	114.3
ITE startup	37.5
ITW cooldown	48.5
Target change	1890.5
Conditioning	708.4
Q-exch stripper	0.2
Subtotal	4574.9
Total	4781.8

Table XXXIII. OLIS beam schedule 105: OLIS beam to ISAC experiments (hours).

Expt	Sched	Actual	Tune	Off	Total
E824	48	6.1	1.0	0.0	7.1
E893	0	0.0	2.3	0.0	2.3
E903	12	1.3	0.5	0.0	1.8
E920	36	9.5	2.8	0.1	12.4
E927	168	43.2	6.5	6.9	56.6
E947	360	238.0	8.7	0.2	246.9
E952	575	385.3	29.8	4.2	419.3
E989	72	84.1	10.5	6.8	101.4
E991	144	78.2	4.7	0.9	83.8
Polarizer	48	95.9	0.0	0.5	96.4
DRAGON	144	96.4	4.8	1.8	103.0
Totals	1607	1038.0	71.6	21.4	1131.0

Total IB experiment time = 2768.1 hours
Combined facility efficiency = 93.1%

Table XXXIV. OLIS beam schedule 105: OLIS systems downtime and overhead.

ISAC systems	Hours
Downtime – unscheduled	
Controls	11.8
Beam lines	5.4
Elec PS	5.0
Magnet PS	26.7
RF controls	3.4
RFQ	0.5
DTL rf	23.7
MEBT rf	18.7
Site power	9.1
Vacuum	19.0
Ion source	81.5
Subtotal	204.8
Downtime – scheduled (overhead)	
ISAC maintenance	175.2
ISAC idle	419.9
ISAC shutdown	540.5
ISAC startup	111.0
ISAC development	702.7
Procedures	419.4
Q-exch stripper	33.4
Subtotal	2402.1
Total	2606.9

Table XXXV. ITW beam schedule 106 (surface ion source targets used: Ta #10 and ZrC #2): September 29 – December 29 (weeks 41–53). ITW beam to ISAC experiments (hours).

Expt	Line	Sched	Actual	Tune	Off	Total
Yield	ILY	168	21.4	0.3	0.0	21.7
E823	8π	132	86.2	0.0	0.0	86.2
E893	LTNO	97	53.3	0.6	0.0	53.9
E956	LTNO	156	93.3	0.2	0.2	93.7
E991	GPS3	0	89.8	0.5	0.8	91.1
E1008	8π	216	78.8	2.5	0.0	81.3
Subtotals		769	422.8	4.1	1.0	427.9
Available					39.4	39.4
Totals		769	422.8	4.1	40.4	467.3

Total RIB experiment time = 467.3 hours
Combined facility efficiency = 78.5%

Table XXXVI. ITW beam schedule 106: ITW systems downtime and overhead.

ISAC systems	Hours
Downtime – unscheduled	
Controls	3.8
Ion source	20.5
Services	21.3
Site power	2.5
Vacuum	80.0
Subtotal	128.1
Downtime – scheduled (overhead)	
Cyclotron maintenance	115.0
Cyclotron development	50.4
Beam line 2A off	81.4
ISAC maintenance	8.0
ISAC development	112.0
ISAC shutdown	288.0
ISAC idle	417.8
Procedures	149.9
Target conditioning	109.9
Target change	247.3
ITW startup	6.2
ITW cooldown	3.7
Subtotal	1589.6
Total	1717.7

Table XXXVII. ITE TM3 beam schedule 106 (Ta #4 target with ECR source and gases; commissioning and development of new facility): ITE beam to ISAC experiments (hours).

Expt	Line	Sched	Actual	Tune	Off	Total
Yield	ILY	24	11.7	0.0	0.0	11.7
E991	GPS3	288	53.9	10.3	1.4	65.6
GPS	GPS1	24	0.0	0.0	0.0	0.0
Subtotals		336	65.6	10.3	1.4	77.3
Available					7.1	7.1
Totals		336	65.6	10.3	8.5	84.4

Total RIB experiment time = 84.4 hours
Combined facility efficiency = 15.6%

Table XXXVIII. ITE TM3 beam schedule 106: ITE systems downtime and overhead.

ISAC systems	Hours
Downtime – unscheduled	
Controls	0.8
Ion source	428.0
Safety	0.5
Vacuum	26.0
Subtotal	455.3
Downtime – scheduled (overhead)	
Cyclotron maintenance	28.0
Cyclotron development	24.0
Beam line 2A off	43.0
ISAC maintenance	60.5
ISAC idle	465.3
Procedures	43.0
Shutdown	288.0
Target change	693.5
Subtotal	1645.3
Total	2100.6

Table XXXIX. OLIS beam schedule 106: OLIS beam to ISAC experiments (hours).

Expt	Line	Sched	Actual	Tune	Off	Total
E893	LTNO	12	0.7	0.0	0.0	0.7
E909	8π	0	3.5	0.0	0.0	3.5
E920	Polarizer	120	48.5	0.0	0.0	48.5
E952	DRAGON	108	42.1	3.9	2.3	48.3
E972	Polarizer	84	46.6	0.9	0.0	47.5
E989	DRAGON	30	6.9	0.0	0.0	6.9
E991	GPS3	276	60.4	2.3	0.0	62.7
E1029	TUDA	36	4.2	0.6	0.5	5.3
DRAGON	DRAGON	121	78.5	4.3	2.6	85.4
8π	8π	0	4.0	0.0	0.0	4.0
Laval	HEBT	228	172.7	0.3	8.0	181.0
Yen	HEBT	12	5.7	0.0	0.0	5.7
Subtotals		1027	473.8	12.3	13.4	499.5
Available					800.2	800.2
Totals		1027	473.8	12.3	813.6	1299.7

Total OLIS experiment time = 1299.7 hours
Combined facility efficiency = 96.4%

Table XL. OLIS beam schedule 106: OLIS systems downtime and overhead.

ISAC systems	Hours
Downtime – unscheduled	
Controls	7.3
Elec PS	4.2
RF controls	6.9
Pre-buncher	0.3
RFQ	2.8
DTL rf	18.4
Services	6.3
Vacuum	0.3
Ion source	2.2
Subtotal	48.7
Downtime – scheduled (overhead)	
ISAC maintenance	50.5
ISAC idle	94.7
ISAC shutdown	288.0
ISAC development	130.8
Procedures	271.1
Q-exch stripper	1.5
Subtotal	836.6
Total	885.3

Table XLI. Summary of overall performance for 2004.

	Schedule 105	Schedule 106	2004
ITW	92.9%	78.5%	89.2%
ITE	74.1%	15.6%	50.6%
OLIS	93.1%	96.4%	94.1%

Table XLII. Summary of beam to experiments for 2004.

Expt	Line	Sched	Beam	Tune	Off	Perf	Type
E816	β-NMR	300	178.7	6.8	2.0	63%	RIB
E817	β-NMR	348	270.6	15.4	16.2	87%	RIB
E823	8π	132	86.2	0.0	0.0	65%	RIB
E824	DRAGON	198	80.0	8.6	2.6	46%	RIB
E871	Osaka	192	191.8	0.9	9.8	100%	RIB
E893	LTNO	97	53.3	0.6	0.0	56%	RIB
E903	Osaka	264	119.6	10.4	0.0	49%	RIB
E909	8π	95	76.3	1.9	6.3	89%	RIB
E920	Polarizer	120	41.7	0.0	0.3	35%	RIB
E921	8π	156	138.7	0.4	19.8	100%	RIB
E956	LTNO	156	93.3	0.2	0.2	60%	RIB
E973	8π	276	170.0	1.0	6.5	64%	RIB
E984	8π	96	67.9	7.2	3.4	82%	RIB
E985	8π	168	189.4	2.6	13.8	100%	RIB
E989	DRAGON	384	180.8	8.1	2.7	50%	RIB
E991	GPS3	480	224.9	13.1	5.7	51%	RIB
E995	ICS	0	15.4	0.0	0.5	100%	RIB
E1008	8π	216	78.8	2.5	0.0	38%	RIB
GPS	GPS1	24	0.0	0.0	0.0	0%	RIB
ICS	ICS	0	8.2	0.0	0.0	100%	RIB
Yield	ILY	1062	155.4	4.4	0.3	15%	RIB
8π	8π	0	4.0	0.0	0.0	100%	SIB
DRAGON	DRAGON	265	174.9	9.1	4.4	71%	SIB
E824	DRAGON	48	6.1	1.0	0.0	15%	SIB
E893	LTNO	12	0.7	2.3	0.0	25%	SIB
E903	Osaka	12	1.3	0.5	0.0	15%	SIB
E909	8π	0	3.5	0.0	0.0	100%	SIB
E920	Polarizer	156	58.0	2.8	0.1	39%	SIB
E921	8π	0	0.0	0.0	0.0	0%	SIB
E927	TUDA	168	43.2	6.5	6.9	34%	SIB
E947	DRAGON	360	238.0	8.7	0.2	69%	SIB
E952	DRAGON	683	427.4	33.7	6.5	68%	SIB
E972	Polarizer	84	46.6	0.9	0.0	57%	SIB
E989	DRAGON	102	91.0	10.5	6.8	100%	SIB
E991	GPS3	420	138.6	7.0	0.9	35%	SIB
E1029	TUDA	36	4.2	0.6	0.5	15%	SIB
Laval	HEBT	228	172.7	0.3	8.0	79%	SIB
LIS	IMS	180	44.1	0.0	0.0	25%	SIB
Polarizer	ILE2	48	95.9	0.0	0.5	100%	SIB
Yen	HEBT	12	5.7	0.0	0.0	48%	SIB

Table XLIII. Isotopic beam delivery for 2004.

TIS nuclide	Hours	OLIS nuclide	Hours
^{6}Li	79.0	^{6}Li	97.1
^{8}Li	516.4	^{7}Li	59.9
^{9}Li	58.2	^{12}C	626.8
^{11}C	20.4	$^{12}C^{3+}$	41.8
^{11}Li	219.2	^{14}N	17.8
^{12}C	1.5	$^{16}O^{4+}$	4.5
^{18}Ne	177.5	^{19}F	124.1
^{19}Ne	5.7	^{20}Ne	43.2
^{20}Na	145.7	^{21}Ne	151.9
^{21}Al	7.8	$^{21}Ne^{5+}$	172.7
^{21}Na	81.8	$^{23}Na^{6+}$	66.4
^{22}Na	1.7	^{26}Mg	40.7
^{23}Ne	2.8	$^{28}Si^{7+}$	6.9
^{24}Ne	3.4	^{139}La	42.1
^{26g}Al	176.0	^{141}Pr	15.9
^{26}Na	145.4		
^{27}Na	42.3		
^{62}Ga	84.4		
^{63}Ga	0.5		
^{64}Ga	0.3		
^{65}Ga	0.2		
^{66}Ga	0.8		
^{69}Ga	44.1		
^{79}Rb	53.3		
^{80}Rb	93.3		
^{130}La	2.2		
^{134}La	39.5		
^{156}Ho	170.0		
^{170}Tm	20.0		
^{172}Lu	37.5		
^{174}Tm	67.4		
^{178}Lu	13.1		
^{174}LuO	0.7		
^{x}Ga	11.4		
^{x}Li	21.7		

The target hall and hot cell operations have become quite well organized. The services in the west MAA were redone to the standard that was set in the east MAA. Careful planning is required to be able to manage the service requirements of the off-line target station during brief maintenance periods in the beam schedule. There were eight target changes done this year, involving all three of the commissioned target modules. Each target change was completed as planned and without incident. In post-operation inspections, three targets were found to have evidence of beam damage: Ta #7 had a hole in the side of the cassette at the central support; Ta #8 had material damage without breach along the side of the cassette; and Ta #9, a high power cassette, had three holes in the front and rear faces. The history of operation of ISAC production targets for 2004 is given in Table XLIV.

Table XLIV. ISAC target history for 2004.

Target ID	In Date	Out Date	Exposure # of protons	Power μA h g/cm^2	Comments
ITW:TM1:Ta #7	09-Mar-04	28-Apr-04	4.53×10^{20}	568,915	28.22 g/cm^2 Ta in the form of 680×0.025 mm foils. Yield low, p-beam had not been centred; hole at cassette support.
ITE:TM3:SiC #7	20-Apr-04	17-Jun-04	6.56×10^{19}	60,373	20.69 g/cm^2 SiC in the form of 460 × 0.26 mm SiC on 0.13 mm C disks.
ITW:TM1:SiC #8	05-May-04	08-Jul-04	4.25×10^{20}	338,864	17.9 g/cm^2 SiC in the form of 375 × 0.26 mm SiC on 0.13 mm C disks.
ITE:TM2:SiC #9	17-Jun-04	11-Aug-04	2.64×10^{20}	205,257	17.5 g/cm^2 SiC in the form of 680 × 0.025 mm foils. Excessive sparking – small external water leak at TGTHTR connection.
ITW:TM1:Ta #8	13-Jul-04	15-Sep-04	5.20×10^{20}	504,438	21.79 g/cm^2 Ta in the form of 525 × 0.025 mm foils. Evidence of beam hitting along side of cassette. No holes.
ITE:TM2:Ta #9	18-Aug-04	27-Oct-04	2.26×10^{20}	219,359	21.79 g/cm^2 Ta in the form of 525 × 0.025 mm foils. High power cassette, yields dropped significantly during operation. Beam too dense – 3 holes in front and rear faces of target.
ITW:TM1:Ta #10	21-Sep-04	18-Nov-04	3.87×10^{20}	374,984	21.79 g/cm^2 Ta in the form of 525 × 0.025 mm foils.
ITE:TM3:$CaZrO_3$ #2	01-Nov-04	26-Nov-04	0	0	1.21 g/cm^2 Ca + 2.76 g/cm^2 Zr + 0.48 g/cm^2 O 6 cm length of CaZrO pellets. No beam due to vacuum leak in ECR coil cooling.
ITW:TM1:ZrC #2	02-Dec-04	02-Feb-05	9.60×10^{19}	90,801	21.25 g/cm^2 Zr + 5.79 g/cm^2 C in the form of 200 ZrC + C composite foils.

ISAC ION SOURCES

Operation of the 2.45 GHz ECRIS at ISAC

A 2.45 GHz ECRIS was built at TRIUMF for on-line applications at the ISAC facility. The source cavity is a single mode TE111 that operates at 2.45 GHz. In order to avoid large containment time the plasma volume is limited using a 12 mm diameter quartz tube located at the centre of the cavity [Jayamanna *et al.*, Rev. Sci. Instrum. **73(2)**, 792 (2002)]. Figure 211 shows a drawing of the ECR ion source and target assembly. The quartz tube lies in the centre of the plasma chamber. The electron cyclotron resonance (ECR) ion source has the following characteristics:

- 2.45 GHz operating frequency,
- Single mode cavity,
- Radial injection of the radio frequency (rf) power,
- No radial magnetic field confinement,
- The axial magnetic field confinement is very shallow. (The magnetic field longitudinal distribution is superimposed onto the mechanical drawing in Fig. 211.)

In May on-line tests with a SiC target were undertaken. The goal was to produce ^{18}Ne for a high precision half-life determination. The ECRIS was operated with the same tune developed during the off-line tests, where a 2% neon ionization efficiency was obtained. A

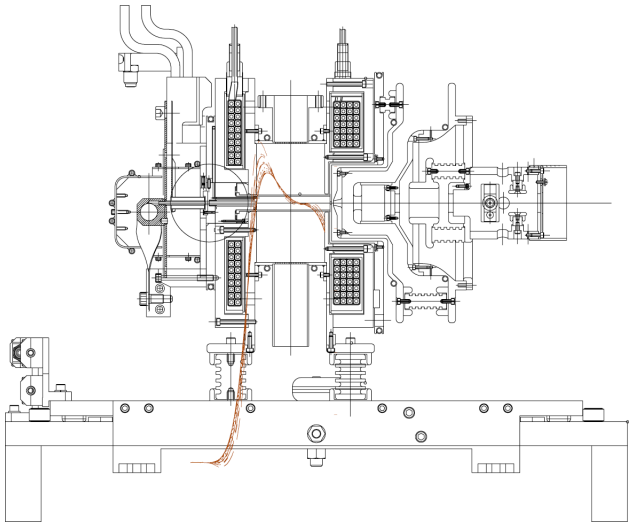

Fig. 211. Drawing of the ECR and target assembly as installed on the tray at the bottom of the target module.

flow of 1 SCCM helium was used as the support gas. The ^{18}Ne yield was measured with 1 μA to 5 μA and followed the proton beam. Above 7 μA the yield did not increase and at 10 μA it was lower than at 5 μA. The on-line neon ionization efficiency was measured and it decreased from 1% at 5 μA to 0.05% at 10 μA.

Furthermore, due to carbon coating of the quartz liner in the plasma chamber, the ECRIS had to run with an Ar-He mixture. The Ar provides a way to reduce the carbon coating on the quartz tube. Unfortunately, the addition of Ar also reduces the ionization efficiency by a factor 3. Figure 212 shows the trend of the ^{18}Ne yield as a function of the proton beam current on target. The dots and squares represent the measured ^{18}Ne yield when the ECRIS was operating with He. The sudden drop at 6 μA corresponds to the addition of the Ar with He as support gas. Then we reduced the amount of injected gas into the ECR. We then changed the support gas from He to Ar. In those conditions we were able to operate the ECRIS with a proton beam up to 30 μA on the SiC target and the ^{18}Ne yield just scaled with the proton beam. The open dots and squares in Fig. 212 show the ^{18}Ne yield when we were operating the ECRIS with only 0.003 SCCM Ar.

During the on-line run we observed that the ionization efficiency was dropping significantly when the proton beam was increased to 10 μA. We changed the support gas from 1 SCCM of He to 0.003 SCCM of Ar only and we were able to maintain the ionization efficiency relatively constant up to 30 μA, which is the nominal beam current we can run on the SiC target.

An on-line run was scheduled in November but unfortunately a water leak in one of the coil cooling circuits was found. The leak rate was such that it was impossible to operate the ion source. An extensive search

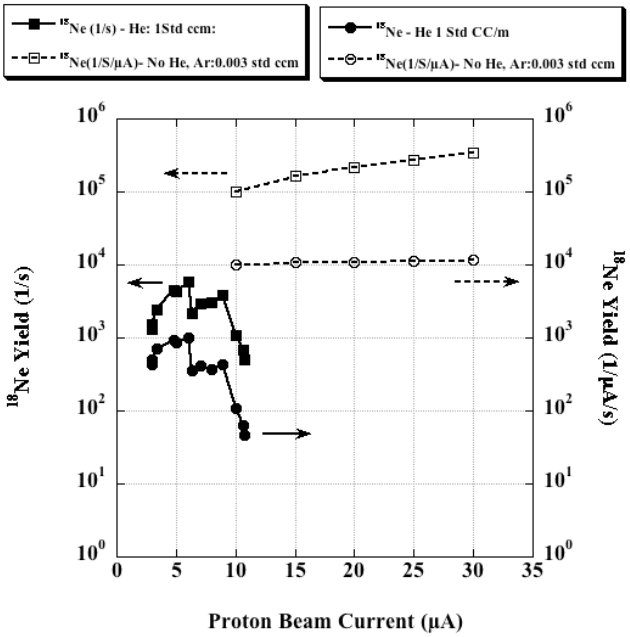

Fig. 212. ^{18}Ne yield as a function of the proton beam current. Solid lines show the ^{18}Ne yield operating the ECRIS with the nominal parameters. The dashed lines show the yield operating the ECRIS without He and only 0.003 SCCM of Ar as support gas.

for the leak was performed during the winter shutdown but did not produce any results. The ECRIS was then put back into the target station vacuum box and once again the leak was confirmed. This time we were able to determine that the water leak was present only if one end of the cooling circuit was hooked to the input. When hooked to the return we did not see the water leak. This was explained in the following way: on the return, the pressure is much smaller than at the supply side (20 psi instead of 120 psi). The ECRIS was then brought back to the hot-cell and the efforts were concentrated on the identified end. The leak was located on one of the water-blocks at a solder joint.

Taking apart the support tray to correct the leak would take too much time so we decided to clog the tiny leak using a vacuum anaerobic sealer that penetrates into the occlusion. A layer of epoxy glue was applied to cover the region. The ECRIS was again brought back into the target station vacuum box and tested. To be on the safe side the two ends of the water-cooling circuit were identified so that we always placed the repaired ends on the return side. Now the ECRIS is ready for a run schedule in May, 2005.

OLIS

Originally OLIS was assembled from parts of I3, only the filaments were removed and a 2400 MHz wave guide installed. When the Y box was installed in 2002 that could accommodate the surface source it was soon

realized that it made servicing of the optics in the original DB2 difficult. Thus in early 2004 DB2 was replaced with a standard LEBT chamber; this allowed the optics of this chamber to be mounted on the chamber lids and thus be quickly removable for cleaning.

Read backs were installed on upstream OLIS skimmers, and on a few downstream of the magnetic bend. They are single gain range and at time of writing will read back a maximum of 30 μA. The reason for this is that the rf source can produce currents greater than 1 mA and it is possible with such large currents to cause damage to optics if there is too much heating or sputtering. These read backs can aid in tuning OLIS and will eventually be used for interlocks or warning should there be changes in the OLIS operating point during experimental runs. Note after mass separation at the magnetic bend the currents are normally greatly reduced.

There was a request for emittance selection slits for OLIS. In December two flanges with 5 mm apertures were installed 1 m apart to reduce the emittance for experiment at the polarizer. This also was to test the idea of improved emittance as an aid to tuning. As it turned out the variation of energy of the OLIS beam was then found to be too large. The original OLIS specifications did not include a precise bias supply, hence the energy variation is greater than that of the target stations.

Table XLV lists the OLIS beams delivered in 2004.

Table XLV. OLIS beams delivered in 2004 (MW means microwave source and SS means surface source).

OLIS	Beam	Facility	Experiment	Start date	End date
MW	^{12}C	DRAGON	Detector	26-Feb	27-Feb
MW	^{12}C	DRAGON	947	01-Mar	15-Mar
SS	^{23}Na	TUDA	927	16-Mar	17-Mar
MW/SS	Various	OPS	Training	22-Mar	26-Mar
MW	^{12}C	DRAGON	952	26-Mar	19-Apr
MW/SS	Various	OPS	Training	26-Apr	27-Apr
MW	Ne	TUDA	927	28-Apr	02-May
SS	Li	TUDA	927	03-May	04-May
MW	^{21}Ne	DRAGON	989	06-May	07-May
MW	^{21}Ne	DRAGON	824	13-May	14-May
MW/SS	La		Dev/920		
MW	^{26}Mg	DRAGON	824	14-Jun	15-Jun
MW	Mg	DRAGON	989	15-Jun	
MW/SS	Mg/Li	DRA/GP3	989/991	24-Jun	25-Jun
MW/SS	Mg/La	DRA/POL	989/920	28-Jun	29-Jun
MW	^{21}Ne	DRAGON	Dev/824	08-Jul	12-Jul
MW	Ne	Osaka	903	13-Jul	
SS	La	Pol	920	15-Jul	
SS	Li		991	01-Sep	07-Sep
MW	F	Pol		16-Sep	21-Sep
MW	Ne	DRAGON		01-Oct	04-Oct
MW	N	LTNO		05-Oct	
SS	Li			06-Oct	18-Oct
MW	^{21}Ne/^{14}N	Laval		21-Oct	25-Oct
SS	Na	DRAGON		28-Oct	31-Oct
MW/SS	La/Pr	Pol	920	05-Nov	09-Nov
MW	^{21}Ne	Laval		12-Nov	15-Nov
MW	^{12}C/^{16}O	DRAGON		18-Nov	22-Nov
MW	F	Pol		01-Dec	06-Dec
SS	Li	Pol		07-Dec	08-Dec
MW	TUDA	TUDA		13-Dec	16-Dec

Charge State Booster (CSB)

The final installation of the charge state booster (CSB) at the ion source test stand has been completed and commissioning of the system started in April. This includes the 1+ line, consisting of an 2.45 GHz ECR ion source, the 14.5 GHz PHOENIX booster and the analyzing system.

In a first series of measurements the CSB has been operated as ECR source only, without injection of 1+ ions, but with a calibrated gas leak of Ar or Ne. The goal was to condition the plasma chamber and the injection and extraction electrode system and to find the operating parameters for the beam optical elements. As an example the charge state distribution obtained for Ar is shown in Fig. 213. For this measurement the source was operated at 100 W microwave power and with a flow of about 10^{-3} SCCM He as a support gas. The maximum in the distribution is at 7+ with an efficiency of 2.7%. Summing up the efficiencies for all charge states leads to a total efficiency of 12%. This includes the transmission of the extraction and analyzing system. Especially in front of the magnet, the high total beam current causes losses due to space charge effects. Additionally, due to the poor vacuum in the analyzer (1×10^{-6} torr), charge exchange for the higher charge states will occur, resulting in an estimated loss of up to 20%.

The emittances for the different charge states of Ar have been determined at the end of the analyzer. Values of up to 20 π mm mrad at 15 kV source potential have been found for 86% of the beam enclosed and no significant dependence on the charge state.

For first charge breeding tests beams of Ne, Ar and Xe have been injected from the 1+ ECR source. Figure 214 shows the efficiencies for the different charge states of Xe. The distribution can be altered by changing the source operating parameters, in this case the microwave power. Most measurements have been done with a very small He gas flow or no support gas. Summing up the efficiencies for the different charge states of Xe results in a total efficiency of 22.5%. In the case of Ar and Ne the maximum in the distribution was at 8+ and 4+ respectively, with a smaller total efficiency, but at this time a microwave power of only 100 W could be used.

The measurements were interrupted in October due to mechanical breakdown of a high voltage insulator. This insulator also supports the inner structure of the source and failed due to mechanical stress, caused by the forces from high magnetic fields. A reinforced replacement has been designed and constructed at TRIUMF. It has been installed and the measurements resumed. First results are that due to improvements in the vacuum inside the plasma chamber the density of

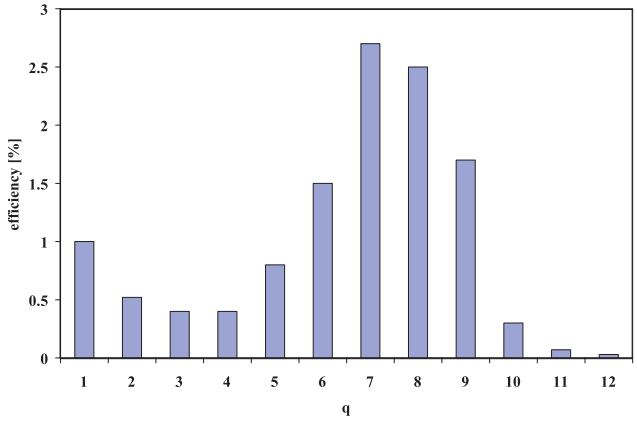

Fig. 213. Charge state distribution of highly charged Ar ions from the CSB. The Ar has been led into the source via a calibrated gas leak.

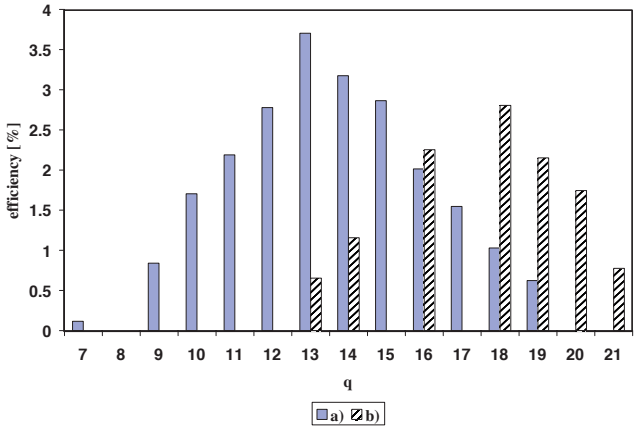

Fig. 214. Charge state distribution of highly charged Xe ions from the CSB. a) $^{129}Xe^{1+}$ injected with 250 W microwave power, b) $^{136}Xe^{1+}$ injected with 320 W.

high energy electrons could be increased resulting in a higher X-ray emission of the source. This makes additional shielding necessary.

Parallel to the measurements a preliminary design study has been made for the installation of the CSB in the ISAC mass separator room. Based on the first results, ion optical simulations have been performed in order to find ways to minimize the losses at the extraction and increase the efficiency. Improvements will be implemented first at the test stand. The design of the final installation will be finished to prepare for the installation in the beginning of 2006.

RIB Development: Resonant Ionization Laser Ion Source

Within the radioactive ion beam (RIB) development at ISAC the TRIUMF resonant ionization laser ion source (TRILIS) continued with on-line installations and off-line beam development for Ga and Al beam production. In summary, TRILIS on-line installations were completed and a development run pro-

vided a beam of radioactive Ga from a SiC target. ^{62}Ga was delivered to 8π (Expt. 823) with a beam intensity enhancement $2\times$ and an augmentation of $20\times$ in the suppression of ^{62}Cu over surface ionization for branching ratio determination. A radioactive beam was successfully produced and delivered for an experiment one year ahead of the initial schedule.

In principle, TRILIS uses multi-step resonant laser excitation and ionization. This technique capitalizes on the potential for element-selective, efficient photo-excitation and ionization, with the major components of the LIS located 20 m away from the radiation area of the target ion source. The basic set-up of TRILIS is shown in Fig. 215 and is identical for off-line development and on-line beam production. In general, RILIS can supply beams of metals and transition elements that are otherwise difficult to obtain. Tunable, high-power, high repetition rate, narrow bandwidth, pulsed lasers are required which can be synchronized with respect to each other. The TiSa laser systems provide above 2 W output power at 10 kHz rep. rate, with typical pulse widths of 40 ns and a spectral line width around 5 GHz. Measured frequency doubling efficiencies are above 20%. Typical excitation schemes employ two and, more commonly, three laser excitation steps for resonant excitation and ionization, with the laser wavelength for the first excitation step usually being in the blue to ultraviolet region of the spectrum. In a typical laser excitation ladder each additional step requires higher spectral energy density. Therefore either Rydberg- or autoionizing-states are best suited for efficient ionization. These states have to be determined experimentally for each element, as only limited spectroscopic information on these high-lying atomic states exists.

Beam development in 2003/04 focused on Ga and preparation of Al beams. Figure 216 details the choice of laser excitation scheme for Ga. In the development work for Ga beams, performed at Mainz University, it became evident that for efficient ionization of Ga, frequency tripling of the TiSa lasers was necessary. Thus, the laser ion source test stand implementation was put on hold, and TiSa laser frequency tripling (planned for 2005) was developed and implemented. Based on the

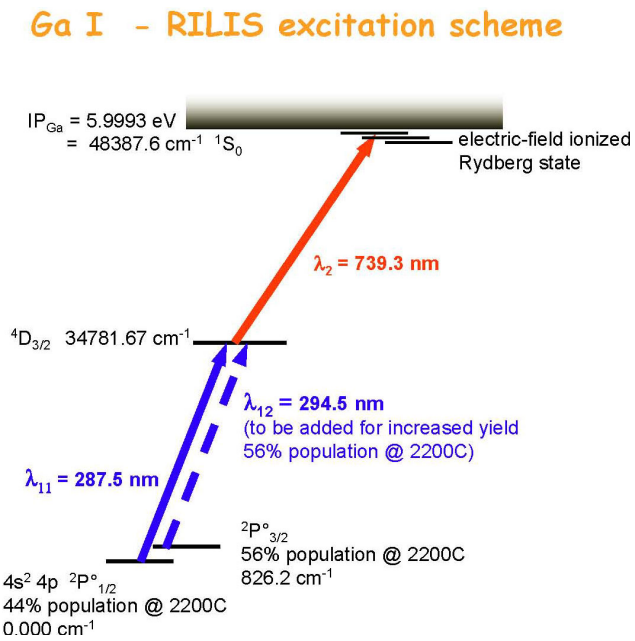

Fig. 216. Two-step resonant laser excitation scheme into a long lived Rydberg state that is subsequently field-ionized. This scheme was the result of detailed development work at TRIUMF and Mainz, and was successfully used for on-line production of ^{62}Ga. For future runs on Ga this scheme will be augmented with a second frequency tripled TiSa laser, to improve yields.

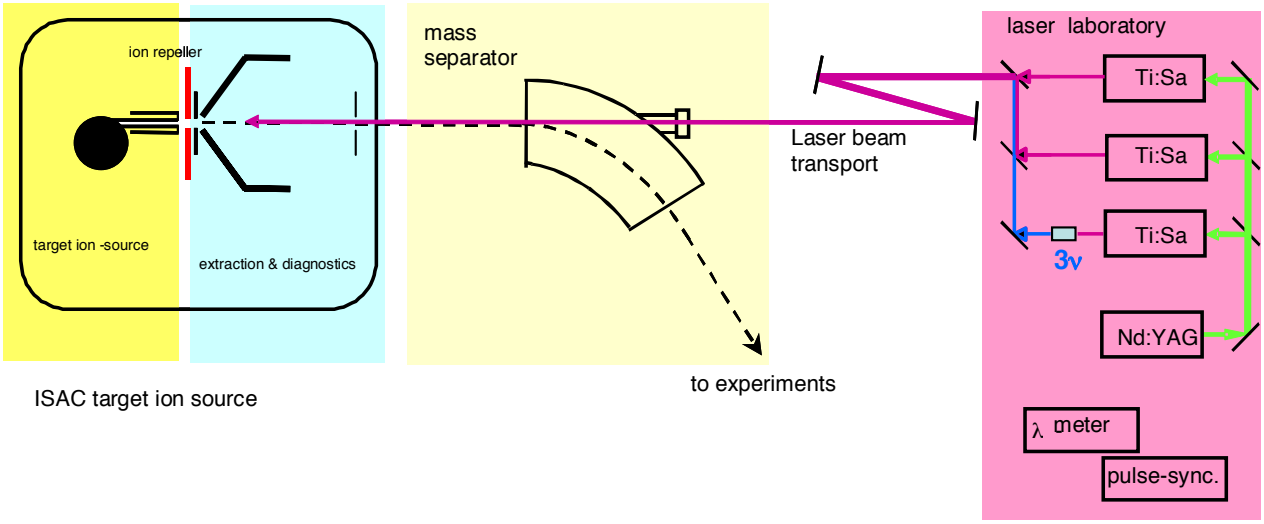

Fig. 215. Schematic of the TRILIS off-line development station with the principal functional groups: target ion source, mass separator and laser system with frequency tripling unit.

design from Mainz University a tripling unit was drawn up, built and used in the first on-line run in December, 2004 providing more than 20 mW at 287 nm. This change in wavelength range also necessitated the installation of additional beam transport opto-mechanics and optics. The complete TRIUMF-Mainz TiSa laser system with frequency tripling as used for the first on-line run is shown in Fig. 217.

Optical alignment of the laser beams into the target transfer tube was done with a transfer tube backed by an optical power meter, both mounted directly on the target module, for direct measurement of laser power in the ionization region.

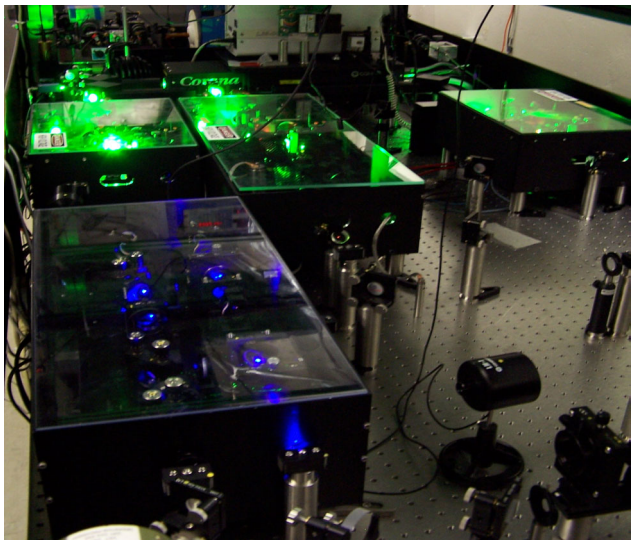

Fig. 217. TRILIS on-line laser laboratory located approximately 20 m from the target ion source. Shown are the wavelength meter, the compact 75 W, 5–25 kHz coherent Corona75 pump laser and the three TRIUMF built Mainz University narrow bandwidth, tunable titanium sapphire (TiSa) lasers together with the prototype frequency tripling unit used in the first TRILIS on-line run.

The development run showed that laser beam transport and beam alignment are of major importance to a successful laser ion source operation. To transport the laser beams into the target ion source, a mock up target module, with optical power meter is now available. This module is installed at the location of the on-line production target, to allow for laser power measurement and initial laser beam alignment. After initial alignment the module is replaced by the actual target ion source, and laser beam pointing stability is visually monitored on a reference target.

In the initial on-line run the laser ion source was continuously monitored by members of the LIS group. Fine tuning of the frequency tripled TiSa laser was performed as an ongoing task, whereas the second TiSa laser did not require any adjustments in the course of one full week of operation. Improvements of controls, monitoring and the laser systems itself are ongoing. For subsequent Ga runs the prototype frequency tripling unit will be replaced by two frequency tripling units, in order to increase yield and isobar suppression. The current status of the collaborative TiSa laser based LIS beam development is summarized in Fig. 218.

The work, installation and first operation of TRILIS was supported substantially by the Mainz group, who also participated with Dr. K. Wendt and Ch. Geppert in both the set-up, as well as the on-line run. Further support was given by the addition of D. Albers, a MSc. student in applied laser technology from FH Ostfriesland in Emden, J.P. Lavoie, MSc. student from Laval University, and T. Achtzehn, Ph.D. student from TU Ilmenau. Also, the enthusiastic support from individuals and groups from TRIUMF is acknowledged and was another key factor to the successful first on-line run.

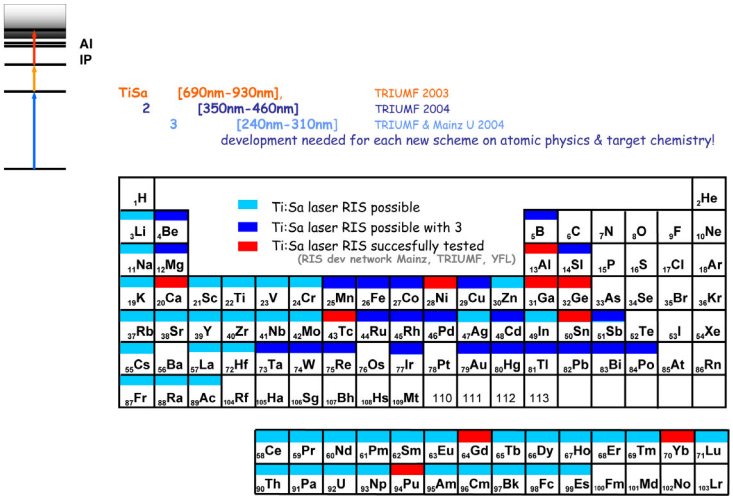

Fig. 218. Status (2004) of TiSa laser based LIS schemes. The development of new beams for laser ion source operation at TRIUMF is to be coordinated through the "beam strategy" group, to coordinate science, proposed experiments, technology and resource issues.

ISAC POLARIZER

All experimental groups that use the polarizer beam line were accommodated this year. The β-NMR/QR group was allotted a total of 5 weeks of polarized ^{8}Li beam time, the Osaka (Minamisono) group was allotted 2 weeks of polarized ^{20}Na and ^{27}Na, and the Osaka (Shimoda) group was allotted 2 weeks of polarized ^{11}Li. The McGill group (Expt. 920) was allotted 1 week of radioactive lanthanum and praseodymium isotopes in the summer and 1 week from OLIS in November. The polarizer beam line and laser systems worked reliably throughout, aside from two brief interruptions due to sodium cell malfunctions. However, other, unrelated problems in the summer shortened the radioactive McGill and Osaka (Shimoda) runs by half. The polarizer dye laser was also run for 4 weeks in September and October, in support of the GSI experiment Expt. 991 that successfully measured the charge radius of ^{11}Li.

We began development of a polarized ^{20}F beam to be used in Expt. 972, which is an extension of the Osaka (Minamisono) group's work on ^{20}Na. All the polarized beams produced to date at ISAC have been alkali metals. In alkali metals the ground state atom has one loosely bound valence electron that can be optically pumped by commonly available lasers. It is not practical to directly pump the ground state of the fluorine atom (or of the ion for that matter), due to the short wavelength light that would be required. A workable fluorine scheme was envisaged based on polarizing the metastable atomic state $3s\,^4P_{5/2}$ via optical pumping on the closed transition $3s\,^4P_{5/2} - 3p\,^4D_{7/2}$ at 686 nm. The metastable state is produced as some fraction of the total atomic beam during neutralization of F^+ in sodium vapour. Its lifetime of 3.7 μs is long enough for an appreciable fraction to survive during the optical pumping process. Collinear laser spectroscopy of ^{19}F was used to investigate the feasibility of the scheme in two OLIS runs in September and December. The aims were 1) to measure the hyperfine splitting of the $^4P_{5/2}$ and $^4D_{7/2}$ energy levels, and 2) to estimate the metastable fraction of the beam. The former is important in devising a practical laser scheme, while the latter determines the maximum beam polarization possible.

The hyperfine structure was determined by observing laser induced fluorescence from the $^4P_{5/2} - {}^4D_{7/2}$ transition while scanning the Doppler-shifted laser excitation frequency (see Fig. 219). The hyperfine magnetic dipole coupling constants of ^{19}F (nuclear spin $I = \frac{1}{2}$) were thus determined for both energy levels. The nuclear magnetic moments of ^{19}F and ^{20}F are known, so the hyperfine structure in ^{20}F ($I = 2$) could be calculated, neglecting shifts caused by the electric

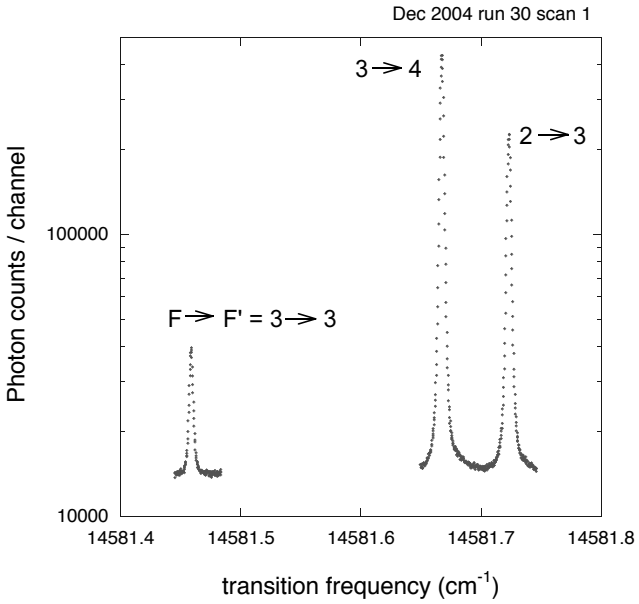

Fig. 219. Laser induced fluorescence showing the hyperfine structure of the $^4P_{5/2} - {}^4D_{7/2}$ transition in ^{19}F. The labels F and F′ refer to the total angular momentum in the lower and upper state, respectively.

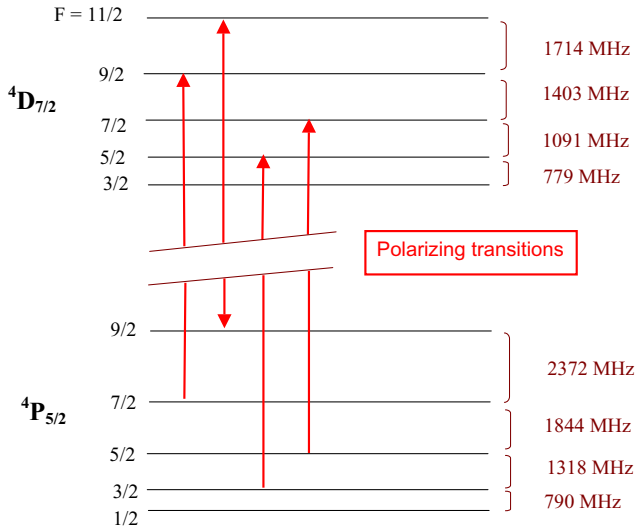

Fig. 220. Calculated hyperfine splitting of $^4P_{5/2}$ and $^4D_{7/2}$ energy levels in ^{20}F.

quadrupole moment (see Fig. 220). It is likely that one laser in combination with a single electro-optic modulator could optically pump most of the metastable population on the strong transitions shown in Fig. 220. This needs to be confirmed with direct measurement of the hyperfine structure of ^{20}F.

The metastable yield was estimated by optically pumping metastable atoms into the ground state via the $3s\,^4P_{5/2} - 3p\,^4D_{5/2}$ transition at 677 nm. The optically pumped beam was ionized in a helium gas cell (as in the operational polarizer) and steered to a Faraday cup. Depletion of the metastable population de-

creased the current observed at the Faraday cup, due to preferential ionization of metastable atoms compared to ground state atoms. The hyperfine structure of the transition was determined by scanning the excitation frequency while chopping the laser beam and using lock-in detection of the Faraday cup current. Then, while sitting on the biggest hyperfine peak, the dc ion currents at the Faraday cup were recorded with the laser "on" and "off". The conclusion was that up to 23% of the ionized beam would be derived from metastables in the limit of zero helium density. One could expect ∼10% ^{20}F polarization in an operational system. Although lower than the typical 50–70% achieved with alkali metal beams, this is still a very useful number. (It could be greatly improved by removing the He cell and substituting UV laser ionization of the $^4D_{7/2}$ state.) We plan at least one more ^{19}F test to investigate the effect of varying the He gas density.

The β-NMR group has requested polarized ^{15}O as a spin-$\frac{1}{2}$ probe that could occupy oxygen sites in high temperature superconductors. Like fluorine, optical pumping must begin from a metastable level, in this case on the closed transition $3s\,^5S_2 - 3p\,^5P_3$ at 777 nm. The fluorine results are encouraging in this regard, since for several reasons the metastable yield should be higher in oxygen:

- The charge exchange reaction that neutralizes oxygen ions in potassium vapour, creating metastable oxygen, has closer to zero energy defect than the analogous reaction between fluorine and sodium vapour.
- The $^5S_2$ metastable level in oxygen has no nearby energy levels to reduce its yield during the charge exchange reaction, unlike metastable fluorine, which has two very short-lived levels $^4P_{3/2,\,1/2}$ nearby.
- Metastable oxygen is so long-lived that decay losses during transit in the polarizer are negligible.

The only disadvantage of oxygen is that preferential ionization of the metastable atom in helium is expected to be slightly less efficient than with fluorine, and therefore less efficient at removing unpolarized background from the ion beam going to experimenters.

ISAC REMOTE HANDLING

The Remote Handling group continued to support ISAC activities throughout the year, servicing the target stations, remote handling of modules and ISAC hot cell operations, along with engineering support in the construction of the latest target module.

The ITW module access area services were fully rebuilt during the winter shutdown with the installation of new cable trays. All new electrical power and controls cabling, as well as new cooling water lines and revised vacuum plumbing were installed. This updating of the west target station will greatly improve service access, reduce risk to services and facilitate contamination control in the area.

Engineering support on ISAC continued with group technicians rebuilding the TM4 target module towards a more conventional arrangement after the unique setup required for the 100 μA target tests completed in 1998. This is now being rebuilt to a standard surface-source configuration for use with high power targets, laser ion source operation or actinide target testing as scheduled in 2005.

The module transport carrier, previously used only for shuttle transport of new modules to the target hall, has been modified both for improved personnel access safety and to provide a vacuum pumping chamber for new module construction leak checking.

ISAC CONTROLS

This year was a "maintenance" year at the ISAC-I control system with no major new system installations. A lot of effort went into peripheral systems, such as TITAN, the charge state booster, etc. During the impending installation of ISAC-II, the group will have to support maintenance of the existing ISAC-I installations without additional manpower. Improvement of tools, which enhance the group's productivity, was therefore given high priority.

As in the years before, the Electronics Development group supplied the hardware support for the ISAC control system, both for design and maintenance.

New Systems

ISAC-II

In preparation for the installation of the ISAC-II systems, which will happen during 2005, the hardware and software structure of the control system was reviewed.

Tests of a new generation of VME CPUs (Pentium based) were concluded successfully. These will be used instead of the 68040 based SBCs used in ISAC-I.

A new system of PLC I/O (Modicon Advantys) was evaluated. This system allows the distribution of I/O modules in small clusters along the beam lines, leading to a substantial reduction in cabling costs and effort. The S-bend transfer beam line between the DTL and the superconducting SCB accelerator will be instrumented with this system. Beam lines in the ISAC-II experimental hall are further candidates.

Advantys I/O was also used for a small PLC system, which was implemented to support the commissioning and the acceptance tests of the Linde helium

liquefier system. Associated EPICS support was provided to allow strip-charting and archiving of selected data.

In order to integrate the Linde system into the ISAC operations, a software driver was written for reading the Siemens PLC, which controls the Linde helium liquefier.

Two group members visited the Canadian Light Source in Saskatoon in order to discuss control system issues, in particular with respect to the Linde helium liquefier plant.

RF amplifier monitoring

Following last year's conceptual design, the system for monitoring all relevant parameters of the 14 ISAC rf amplifiers was produced. PLC drops for all amplifiers, using the distributed Advantys I/O system, were built for 10 amplifiers. The system is ready for installation, but is waiting for parts delivery for signal conditioning boards.

Integration of ISAC building controls

The ISAC building control system is a commercial system, using the BACNET network protocol for communication between devices and supervising PC workstations. This system stands alone, does not provide satisfactory data archiving facilities, and suffers from a host of operational insufficiencies.

A major project was begun to integrate this facility into the ISAC control system. The starting point was open-source BACNET drivers for Linux, which were essentially alpha state. These drivers were debugged and made functional. A BACNET application was developed, which allows fast startup of the monitoring system from a locally stored database. This local database is acquired by lengthy on-line exploration of the installed system. The BACNET application was interfaced to an EPICS soft IOC running on the same Linux machine. This will allow monitoring of all building control parameters through the ISAC control system.

The BACNET/soft IOC combination is undergoing final testing at the moment.

Functionality Enhancements

ISAC-I diagnostics

Software drivers for the VQSX beam current amplifiers were upgraded to provide auto-ranging and logarithmic output capability.

In the IOS section, software support for a new set of beam skimmers was implemented.

CAN-bus based beam current integrators were installed at some Faraday cups in the IMS, 8π, and TUDA beam lines in order to increase readout sensitivity.

Charge state booster

At the ion source test stand, the control system for the charge state booster was completed. Support for all beam diagnostics elements was implemented. Beam current amplifiers with higher current capability were installed. A new water flow controller box with analogue flow read-out was added to the system. Control of the CSB power supplies was moved from CAN-bus to the PLC, in order to support a changed interlock specification. The PLC interlock system was enhanced in software and hardware to allow the CSB HV to be run independently from the ion source or from a common HV supply. MATLAB applications for better visualization of emittance scans and correlation plots were developed.

TITAN RF cooler

The components of the TITAN control system were implemented and commissioned. This included the new rf cooler optics, which uses TRIUMF developed VME-based voltage supplies. An EPICS operator interface was supplied. EPICS driver and device support for the TITAN-specific VME modules was enhanced and commissioned.

ISAC-II cryomodule

Ongoing support was given to the SCRF facility. The EPICS interface to the rf control system was changed. The unstable portable channel access server was replaced with a "soft IOC", a new software tool, which became available with EPICS release 3.14. The soft IOC was interfaced to the rf controls with a software "glue" layer based on a shared memory protocol. This upgrade improved the stability of the system dramatically. It will be used for ISAC-II and should also be retro-fitted to the ISAC-I rf controls if time and resources permit.

A similar soft IOC was integrated with the commercial Windows-based system for cavity alignment. This gives the alignment system access to EPICS facilities like archiving and strip-charting of data.

Target conditioning box

At the target conditioning box, many small modifications were made to support changing requirements for testing of the laser ion source, high current targets, and the development of a FEBIAD source.

Miscellaneous

Changes were made to the PLC software to implement "soft" roughing of several diagnostics boxes in the HEBT sections.

In order to make IOC development easier, separate small PC104-based IOCs were deployed for the supervision of the evaporator, TIGRESS detector fill, and M9/M15 vacuum system PLCs.

At the laser ion source, a Windows-based PC runs a commercial software package to read and process wavemeter data. A soft IOC was provided to allow data visualization and logging by EPICS.

Experiment Support

PLC and EPICS support was implemented for Expt. 991 at the end of the ILE2 beam line.

Temporary modifications were made in the ILE2 polarizer section to accommodate Expt. 990.

For DRAGON, the PLC program was enhanced to support new devices and configuration change between different detector systems at the end chamber.

System Support

System maintenance on the development and production nodes occupies an ever increasing amount of time. In addition to the console machines, there are now 9 Solaris servers, 4 Linux servers, and 4 Linux firewalls.

The protection of all EPICS based control systems with firewalls was finished. The production machine(s), IOC(s), and PLC(s) are grouped behind separate firewalls for

- ISAC
- Ion source test stand and TITAN
- SCRF, target conditioning station, evaporator.

In addition, a firewall protects the development systems in Trailer GgExt.

The EPICS CA gateway program was installed on a Linux machine with the intent to concentrate all user connections to IOCs, thereby reducing the network and memory load on the IOCs. This led to the discovery of serious bugs in the gateway software, which was reported back to the EPICS collaboration. Until a fix is available, the system was reverted to the previous configuration.

EPICS auto-save/restore routines were modified to use the IOC's NVRAM, and installed on some IOCs to allow bumpless reboots.

The logging configuration of the EPICS IOCs was reconfigured. A separate IOC log server for each IOC accepts console output logging and writes to a set of rotating logs. CA output logging, the operator activity log, is handled by a dedicated IOC log server.

Two new SUN servers were acquired to replace two mission-critical servers, which had been in faultless operation since 1997. One of the new servers failed catastrophically in December. This exposed a weakness in our server redundancy configuration. Bringing the backup server on-line required more intervention of a system expert than expected. As a consequence, a new server hot-sparing concept is being implemented.

All production servers were relocated to the ISAC-II controls development room.

All IOCs were upgraded to EPICS release 3.13.10. The new EPICS release 3.14 was compiled and used for support of soft IOCs and the CA gateway. All ISAC device drivers were modified to support 3.14. No decision has been made yet to upgrade to 3.14.

Development and QA Support

Device database

The ISAC control system relational database and associated Web-application was further enhanced to include more checking tools. IOC configuration and roll-back was refined, CAN-device configuration was included, Capfast symbol import was improved, and a better device name aliasing system was implemented.

Perl tools were written to support PLC interlock checking and device control panel building for the Concept PLC programming software, which is used with the new Advantys I/O systems.

NCR system

A new version of the Web-based ISAC fault report system was designed and implemented following specifications by the ISAC Operations group. The new "non-conformance reporting" (NCR) system uses the PostgreSQL relational database system as back-end. The system complies with the TRIUMF QA program and supports the full life-cycle of an NCR.

Bypass and force tracking

New tools were developed in order to improve tracking of interlock bypasses and device forces. Issuing of bypass and force commands to the control system is now limited to operators. The reasons for bypasses and forces are tracked in a relational database, so that status and history can be easily queried.

Operation

In general, operation of the control system during 2004 was not too eventful. There are still too many IOC reboots required to revive "hung" IOCs. These reboots usually do not cause loss of beam, but are a nuisance nevertheless. Reasons for the hang-ups are task crashes on the IOC or starvation of resources. Due to the intermittent nature of these problems, progress in addressing them has been slow.

VACUUM

ISAC-I

The Vacuum group maintained and repaired the vacuum equipment on accelerators and the beam transfer lines. Assistance was provided with setting up vacuum systems for different experiments by GSI, Laval University, etc. on GPS2, GPS3 and on the end of the HEBT. The last vacuum section of 8π has been

upgraded with a Varian dry Scroll 300 mechanical pump. The vacuum diagram was produced for the TITAN/RFQ cooler, and two V-1000 turbo pumps were repaired also for TITAN. The Vacuum group assisted the CS-booster development with vacuum services.

Targets

Both target stations performed well during the year, at an average vacuum of about 8.0×10^{-7} torr. Diaphragm gauges were installed on decay and operating storage tanks for better vacuum monitoring. The diaphragm gauge is not a gas-dependent type as is the convectron. The failure of a hermetically-sealed mechanical pump required the installation of the spare. The second hermetically-sealed pump was also replaced as a preventive maintenance precaution. Replacement pumps have been ordered. Two Varian V-1000 turbomolecular pumps failed during the year and both have been replaced with new pumps. The faulty pumps had bearings replaced and rebalancing done. The Penning gauges had stability problems related to controllers, grounding and due to work in excessive outgassing during target initial bake out. The Vacuum group looked after retrieving samples from the decay storage tank for survey before each gas removal. The group has also been involved in intensive leak checking of heat shield cooling lines for target module #1 and the ECR target module.

Mass separator area

A few tests have been done with the goal to find a way of improving vacuum in between the mass separator and RFQ for the beams with a high charge transfer. The cryopump and electrical tape heaters have been installed for the test. The data obtained is compatible with ISIS experience with cryopumps. The baking with heaters to reasonable (about 50–60°C) temperatures did not change the vacuum. Two convectron gauges were replaced on the mass separator platform. The baking mechanical pump on the platform had a complete overhaul several times during the year. The quick oil quality degradation has been noted.

LEBT

The Varian turbo pump V-551 on the polarimeter has been replaced as well as turbo pumps ILE2:TP21 and ILE1:TP10. One turbo pump controller has been repaired. Two mechanical pumps have been replaced.

RFQ

The water cooling has been added to all RFQ Leybold turbo pumps.

DTL

The DTL roughing pump has been repaired.

HEBT

Installation of the S-bend take off dipole magnet with vacuum chamber is scheduled for the winter shutdown. The HEBT vacuum system modification is planned for the same time. The modification will involve the splitting of the vacuum system into separate sub-systems with separate roughing/backing pumps in each sub-section. This will shorten the pump downtime and will simplify control system interlocks.

The cold finger cryopump has been maintained and the new high pressure helium lines were installed. Two ion gauges, one mechanical pump, and one turbo pump controller have also been replaced.

ISAC-II

Vacuum and cryogenics

The Vacuum group assisted the ISAC-II project with vacuum and cryogenic services in the SC Linac development and the S-bend. A lot of leak checking was done on cryomodule components during manufacturing, and cold tests were performed on the first cryomodule. A 1000 l helium dewar, manufactured by CRYOFAB in 1983, has been restored and installed as a part of the helium refrigeration system. The current leads for the SC-solenoid have been designed and assembled.

Liquid helium and liquid nitrogen

The Vacuum group is looking after liquid helium and liquid nitrogen deliveries and distribution on site.

The new 9000 US gallon nitrogen tank replaced the smaller tank located by the east wall of the ISAC-I building. It is serving users connected through the ISAC-II nitrogen distribution system and portable dewar fill station inside ISAC-I.

The old helium refrigerator, which occupied space in the helium building, has been sold.

The Linde TCF-50 helium refrigerator system is under construction with commissioning scheduled for February–March, 2005.

ISAC-I RF SYSTEMS

ISAC rf systems performed very well over 2004 with availability of about 97% and total downtime of 81 hours.

LEBT Pre-buncher

The LEBT pre-buncher was routinely operated to bunch the dc beam in the LEBT into a desired bunch structure for injection into RFQ. The rf amplifier misbehaved twice. The first time it was a solder joint failure of one of the resistors in the amplifier module. The second time was a loose rf connector failure. Both troubles caused beam instabilities.

RFQ

The RFQ operated well in 2004, and system downtime was mainly associated with the computer control system. Major developments done on the RFQ system were:

- RF control computer and VXI control system were powered from a UPS;
- Cooling circuits of tuners, coupler and tank structure were refurbished to incorporate water flow controls and interlock;
- All 6 RFQ vacuum turbo pumps were equipped with water cooling;
- An updated version of the anode power supply soft start circuit board has been manufactured and commissioned into the system;
- RF controls hardware was modified to perform the frequency tuner initial position alignment. Corresponding software upgrade is under way.

Bunch Rotator

The MEBT 105 MHz bunch rotator was routinely used in operation to achieve the desired beam quality.

During the winter shutdown the bunch rotator cavity was taken off-line and dismantled to investigate the problem of multipactor discharge, which made the startup procedure rather difficult. A visual inspection revealed a few areas with multipactor marks around the stem and rings. A surface coating with Ti to reduce secondary electron emission was considered and rejected due to unacceptable impact on the beam schedule. Instead we painted the troublesome areas with Aquadag (see Fig. 221). In the past this kind of treatment had been proven to reduce the multipactoring in the main cyclotron rf structure. After Aquadag treatment the rotator cavity was tested at a test bench at signal and high power levels. An improvement in conditioning time has been achieved, though we were not able to completely suppress multipactor discharge.

A new, smaller coupling loop was installed for the cavity, which significantly reduced the capacitive coupling and improved system stability. To compensate the frequency shift introduced by smaller coupling loops, a 5 cm diameter tuner plate was used to replace the existing 3.8 cm one.

An amplifier tetrode tube degraded in performance with an indication of aging, though it has operated only about 4000 hours. A spare 3CX 3000 tube was installed and easily gave 5 kW output power (required power is 2.6 kW). To increase tube lifetime, the filament voltage was reduced from 7.7 V to 6.8 V after the tube was conditioned for 200 hours.

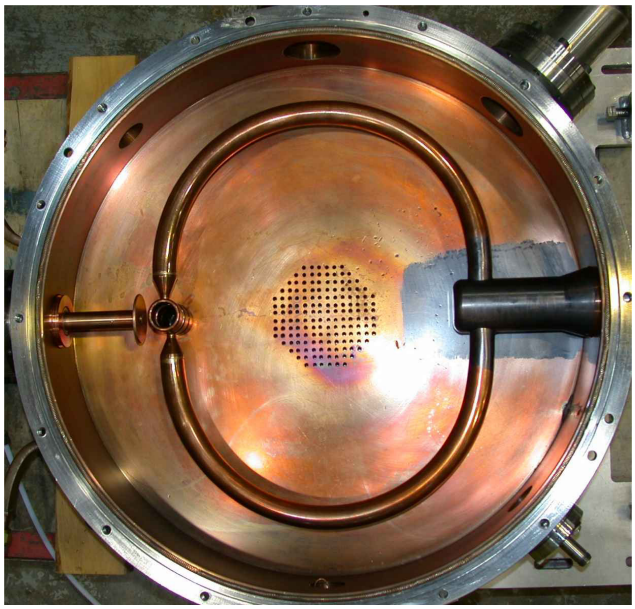

Fig. 221. MEBT bunch rotator painted with Aquadag.

MEBT Rebuncher

The MEBT rebuncher operated very reliably this year. The rebuncher cavity was tested to operate without endplate cooling and the frequency tuner taken out of regulation loop. Despite these changes the system has shown stable operation without any trouble during the year.

DTL

Due to cooling water pollution coming from rusting steel endplates, the DTL tank #1 had also gone through a similar test in 2003. We had run it at nominal rf power (4 kW) without endplate cooling. Structure temperature rapidly rose and the fine tuner could not compensate frequency change due to the tuning range limit. Subsequently an external water-cooling of the endplates had to be implemented instead of original internal cooling. In June, 2004 we installed 4 detachable heat sinks to both endplates. The system has operated well ever since. Recent investigation on the deionized water quality has not revealed any contaminates in the return circuits.

In January there was an incident, when DTL tank #4 was tested at high rf power while the DTL cage was open and accessible to personnel. An investigating committee has identified some deficiencies in the procedures which caused a failure in the hardware (interlock relay). Following committee recommendations, the DTL cage safety interlock has been upgraded during last year. The trip signals of X-ray or high rf levels should now turn off all DTL rf driver and screen power supplies. The trip status is latched in the safety system and in the rf amplifier controls. The rf amplifiers can

be powered again only after clearing and resetting the interlock status. The interlock status is now displayed at the DTL rf control consoles, advising the operator about DTL cage safety status.

DTL amplifiers

After extensive maintenance in 2002 the DTL amplifiers did not require any specific service over the past two years and worked very reliably. The only failure was in the DTL tank #1 PA. A homemade anode blocking capacitor experienced a destructive spark, which produced a 2 mm diameter hole in the kapton insulator. A broken capacitor was replaced with a spare one.

The amplifier remote control system was developed. New data processing and interface boards are housed in the shielded metal boxes in each of the 8 DTL amplifiers. Adequate HV protection and rf filtering are incorporated into the design. All PA voltages, currents and status signals are provided to the ISAC main control system via a PLC. An EPICS control page is being developed. The amplifier hardware upgrade included installation of new 3 ft Tx-line directional couplers, rf driver 1 kW directional couplers, rectifiers, voltage dividers, current sensors, and associated wiring. Final commissioning of the remote control systems for all 8 DTL PAs is planned for spring, 2005. Control systems for the rest of the PAs will be upgraded afterwards.

HEBT High Beta Buncher

Following the test results of 2003, the upgrade of the frequency tuner for the 35 MHz buncher has been completed during the winter shutdown. A modified tuner does not comprise rf fingerstocks, which rapidly deteriorated due to friction in the past. Removal of finger contacts caused resonant frequency shift, which was adjusted by means of the coarse tuner. The fine tuner new operational range covers cavity detuning due to heating by rf power in the full working range from 0.5 to 13 kW. Maximum heat dissipation on the tuner itself leads to an insignificant temperature increase of 15°C. The new tuner is interchangeable with DTL tank 2, 3, 4 and 5 tuners. This reduces the required number of spare parts for the rf system.

RF Controls

Over the year the RF Controls group regularly provided routine tune up of the rf control system. A number of spare rf control boards for different frequencies of the ISAC rf systems have been tested during shutdown time.

ISAC DIAGNOSTICS

Cryomodule Alignment Hardware

The ISAC-II superconducting cavities must remain aligned at liquid He temperatures: cavities to ± 400 μm and solenoids ± 200 μm after a vertical contraction of $\sim$4 mm. A wire position monitor (WPM) system based on a TESLA design has been developed, built, and tested with the prototype cryomodule. The system is based on the measurement of signals induced in pickups by a 215 MHz signal carried by a wire through the WPMs. The 0.5 mm diameter copper-bronze wire is stretched between the warm tank walls parallel to the beam axis providing a position reference. The sensors, one per cavity and two per solenoid, were attached to the cold elements to monitor their motion during prealignment, pumping and cool down. A WPM consists of four 50 Ω striplines spaced 90° apart. A GaAs multiplexer scanned the WPMs and a Bergoz card converted the rf signals to dc X and Y voltages. National Instruments I/O cards read the dc signals. The data acquisition is based on a PC running LabVIEW. System accuracy is $\sim$7 μm.

Alpha Acceleration Hardware

For the experiment on acceleration of alpha particles from a radioactive source in superconducting cavities, a ^{244}Cm source with an intensity of 10^7 Bq was attached to the upstream diagnostics box on the front of the cryomodule. In order to prevent possible contamination, the source was separated from the cryomodule vacuum by an 8 μm kapton window of 2 mm diameter and a copper mesh screen. The detector consisted of a silicon surface barrier detector in a vacuum box connected to the downstream end of the cryomodule. The source and detector could be valved off and a magnet could be turned on to sweep away electrons from the cryomodule before reaching the detector. The absolute measurement of the energy of the accelerated alphas was crucial. To calibrate the detector, a low level alpha source could be moved in front of it. It produced a spectrum of three lines between 5 and 6 MeV and consisted of a mixture of isotopes: ^{239}Pu, ^{241}Am and ^{244}Cm. It was found that the cavity tuner motors induced significant switching noise despite the use of double shielded signal cables. To alleviate the noise, the detector ground was floated and the pre-amp moved close to the detector. The electronics was standard: an +80 V bias supply for the detector, a charge-sensitive preamplifier, a pulse amplifier. The alpha particle spectra were collected by a multichannel analyzer and read by a laptop running acquisition software under LabVIEW.

Stripline FFC

A fast Faraday cup (FFC) in the diagnostics box of the cryomodule will be used to tune the buncher in the new transfer line to ISAC-II. The existing FFCs are too long in the beam direction, ∼6 cm, for this location. A thinner, ∼2 cm, FFC was designed based on a water cooled ceramic printed circuit board (pcb). A biased screen in front of the pickup electrode shields it from the EM wave which precedes the ion bunch, yielding a fast time response. A fine copper mesh screen was supported by a 0.5 mm spacer in front of the electrode and this assembly was soldered to a separate track on the pcb. The device was tested

Other Activities

Certain attention was given to the diagnostics capable of monitoring beams with intensities from a few to 10^6–10^7 ions per second. Current emphasis is placed on two types of devices: secondary electron emission monitors (SEM) and CVD diamond detectors. Both detector types are considered radiation hard and, therefore, suitable for beam diagnostics purposes. They will be used complementary depending on requests and experimental conditions and, hopefully, will satisfy current demands on "low-intensity" diagnostics. It should be noted that in contrast to the SEMs, diamond detectors will require additional R&D but are potentially very attractive since they are very robust and simple in operation. Two detector grade CVD diamond wafers from Element Six Ltd. have been acquired for prototyping. Several devices of both types will be developed and built in the upcoming year.

The vacuum stand for testing detectors and other equipment is complete. The multipurpose diagnostics box arrived from the shop at the end of the year and successfully underwent vacuum leak tests. The final assembly was delayed in connection with a decision to replace the existing roughing pump with an oil-free scroll pump to prevent contamination and eventual damage of sensible detectors, e.g. microchannel plates. The pump is currently being commissioned.

ISAC-I CONVENTIONAL FACILITIES AND INFRASTRUCTURE

Two significant failures tarnished what would have otherwise been a relatively quiet year. A required upgrade in chiller #2 was postponed due to financial constraints. Regular engineering support continued to be provided to users on electrical and mechanical services matters. This included participation in engineering design reviews for accelerator as well as experimental facilities, cost estimating, services design and specification, procurement and installation supervision as well as attending to operational problems and maintenance.

Preliminary work started on TITAN and β-NQR services design. A review of the CSB services requirements indicated that they could be housed in the mechanical room next to the mass separator vault. Safety interlocks for the 8π experimental facility obtained final approval of the engineering review panel. They will be installed next spring.

A number of improvements were brought about. The overload of the LEBT 208 V power distribution was resolved and the local capacity expanded to accommodate an increased demand in the area. A safety concern with one of the main LEBT cable trays was attended to. A water leak in the electrical room was fixed and the feeder to DTL tank 5 was increased. UPS power was supplied to the RFQ controls that were experiencing too frequent nuisance trips.

The most important maintenance activity was the replacement of both variable frequency drives (VFD) and motors for both cooling tower units in late October. This equipment has been in service for about 8 years. The cooling tower system is critical to the continuing operation of ISAC and is required to be highly reliable. We have experienced serious problems in finding replacement parts when the first unit failed, but the problem became critical when the second unit failed. We were left with little support from the manufacturer's local service representative. Our vulnerability to the outside service support was evident. After a careful review of the technical problems and the required reliability, the decision was made to change manufacturer of the VFD. We also improved on the previous design to better protect the motors from the damaging effects of impulses created internally to the VFD. Chokes were added to both line and load side. The first unit was commissioned early in November. The reliability of the VFD from the same manufacturer installed in the radiation exhaust system came into closer scrutiny as more frequent troubles were reported. In the process, we decided to replace in time that VFD as well. This task is planned for next year. Another major failure occurred in one of the uninterruptible power supply units, when one of its inverter's card burned. UPS reliability and availability are also critical to continuing ISAC operation. The repair of these units is expensive and we are looking at replacing the whole UPS system with a more reliable one.

About 22 installation orders were processed for ISAC-I, amongst them services to Expt. 991, TITAN test stand, TRINAT lasers and DTL-8 amplifier.

Mechanical Services

Several large projects dominated activity. The NALCW system for ISAC-II was started up and provided water to its first consumer, the rf test stand. Be-

cause of the contamination of the mains in ISAC-II for this system during construction, cleaning and repeated flushing was required before water could be allowed to return to ISAC-I. After water was allowed to flow, the return water to ISAC-I was filtered for several weeks to ensure all loose materials were captured. One casualty was the de-ionizing resin which faithfully polished the new piping system before expiring. After having to polish the ISAC-I piping and five more years of service it was near the end anyway.

ISAC-I room 06 (actinide lab) fume hoods had HEPA filters installed which required new ductwork squeezed into the tight space available, exhaust fan speed up, installation of a new fume hood, and repiping of services including changing the cup sink drains from the active to the sanitary system.

The cryogenics project called for action on several fronts. Room 164 required rotation of the existing ventilation fan, relocation of a sprinkler main, and installation of water and air piping. In the helium compressor building the existing fans were removed and a new roof top system installed to meet the high demand for compressor ventilation. A new flow switch was installed in the incoming sprinkler line to alert controls in the event of a fire.

A compromise design exhaust fan was installed in each of the glass enclosed stairwells. Compressed air service was provided to room 03. MRO work included TRINAT heating coils and piping modifications, and a new radio operation system for the ISAC-I experimental hall crane.

ISAC PLANNING

This year the Planning group was involved in planning, scheduling, coordinating and expediting several sub-projects for ISAC-II (medium beta cavities, wire position monitor, cryogenics system, high beta cavities, charge state booster, HEBT transfer, H-HEBT, ECR); planning and coordinating activities for two shutdowns (December 22 – mid April and September 13 – October 6); ISAC experimental facilities (TIGRESS, TITAN); and M20Q1, Q2 refurbishing.

Technical details and progress on PERTed activities are described elsewhere in this Annual Report under the respective principal group. However, following is a summary of the main projects along with the major milestones achieved.

ISAC-I

Various plans and PERTs were prepared and updated regularly with manpower estimates and analysis to identify critical areas and resolve any problems. ISAC priorities were evaluated and higher priority was assigned where necessary to optimize the scientific output and meet overall milestones.

ISAC-II

Medium beta cavities

The remaining cavities, #8–20, were fabricated, inspected, chemically treated and received at TRIUMF. Cavities for the first two cryomodules (SCB3 and SCB1) were cold tested, with the remaining cavities to be tested by May, 2005. The cold test results indicated that three flat type cavities (#7,9,12) did not meet our quality specifications. The plan is to electro polish cavity #7 at Argonne for now in order to resolve this quality issue and establish an agreement with Jefferson Lab to chemically treat our cavities as needed. Tuners and coupling loops for the first 2 cryomodules have been received and are prepared for installation. The remaining components are expected to arrive early in 2005. Cryomodule tanks 2 and 3 were received and the LN_2 shielding fabricated and installed in the tanks. Cold tests and rf tests on cryomodule SCB3 were completed in November, and the assembly of cryomodule SCB1 started in December with an aim to move it to the clean room in February, 2005. Considerable effort was put in by the machine shop to fabricate the components for cryomodules SCB1 and 2. Cold tests and rf tests on cryomodules SCB1 and 2 will still require extensive expediting of components and appropriate manpower allocations to meet the scheduled completion dates. As an intermediate milestone, the plan is to test SCB1 with final cabling, rf controls and configuration by June, 2005. The plan is to install the last cryomodule #5 and be ready for beam in December, 2005. The fabrication of components for SCB4 and 5 was delayed to the 2005/06 fiscal year due to budget constraints.

Cryogenics system

Process and instrumentation drawings (PID) were completed which specified all the components required. The contract for the cold box, compressor/ORS and He ambient vapourizer was awarded in November, 2003 to Linde. These components began arriving at TRIUMF on schedule in July and September, 2004. After an extensive search the buffer tank was procured, cleaned, leak checked and installed on its pad in October. The plan is to install refrigeration systems and distribution systems in early 2005 with the overall system commissioning by Linde in March, 2005.

High beta cavities

Preliminary physics specs for the high beta systems were completed by December with an aim to review the initial conceptual design to finalize the decision regarding the cavity frequency by March, 2005. The aim is to finalize the design followed by an evaluation of a local company for manufacturing cavities, and then

fabrication, testing and evaluation of a prototype cavity by March, 2006. The specifications of all cavities can then be finalized and the fabrication order will be placed. The plan is to complete the high beta system by summer, 2008.

Charge state booster (CSB)

ECR mode and breeding mode commissioning continued in 2004. Several tests had to be done to specify the shielding required for X-rays. Tests with the rf cooler will take place in spring, 2005, and optimization will continue until the end of the year when the CSB will be ready to move to its final location. After the rf cooler tests are complete, optics design will begin for the CSB implementation in the mass separator room due to required shielding constraints. The aim is to have all the components fabricated and assembled and prepare for installation in the January, 2006 shutdown.

HEBT transfer line

Many components for the HEBT transfer line were fabricated and procured during 2004. Two of the four dipoles were received in June. The other two needed repairs, were sent back to Alpha, and were received in August. The main support frame, service trays and racks were installed by August. The rebuncher was received at TRIUMF, and assembly of the components onto the rebuncher continued with an aim to be ready to install in the DSC line after the January, 2005 shutdown. Installation of all the components continued up to December, 2004. The plan is to install MB0 with its associated vacuum system, services and controls and connect with ISAC-I HEBT during the January, 2005 shutdown.

H-HEBT

Physics specifications of the H-HEBT have begun with the aim to have the layout finalized by February, 2005, after which the design and fabrication of the components will begin. The plan is to have the vault section of the H-HEBT ready for beam by December, 2005, and finish the installation into the first experimental station by April, 2006.

TIGRESS

The stand and substructure for one detector were fabricated and all the related electronics, readout systems and electronics for the prototype substructure were ordered and procured. The prototype substructure was tested in June, and as a result a new front suppressor block was designed in December. The new block will be installed in January, 2005 and new test results will be analyzed and evaluated with an aim to then be able to start on the design of the components for the remaining 4 detectors in May, 2005.

The optics design of the beam line has been completed and the overall engineering design will commence after May, 2005. The aim is to have all the beam line components assembled and installed and ready for beam in August, 2006.

TITAN

The TITAN platform was designed and ordered in December. It will be fabricated and then will be installed in location during the January, 2005 shutdown. Tests on the rf cooler in the proton hall started in the summer and will continue up to spring, 2005. The plan is to move it for tests with CSB in the test stand in May, 2005. The EBIT is being fabricated, assembled and tested in Heidelberg, Germany with the plan to be ready to ship to TRIUMF in the spring, 2005. The Wien filter has been received from McGill and is being prepared for installation on the platform. The transfer beam line system has been designed and fabrication began in the fall. The aim is to be able to install the transfer beam line in June, 2005. The Penning trap has been designed, and the superconducting magnet ordered. Design work will continue on the Penning trap components up to spring, 2005. The overall plan is to be able to install all the components on the platform and be ready for experiments by the end of 2005.

Actinide Target Test

A task force was formed to define the overall project scope with an aim to do preliminary tests and prepare a safety report for CNSC to get a license to do tests with RIB. A work breakdown structure was developed and the major subprojects included: alpha monitoring system, hot lab and target preparations and hot cell modifications. The project progress was slow in 2004 due to the longer time required to answer many outstanding questions in order to start proper engineering conceptual design.

Shutdown Activities

There were two shutdowns during the year: the winter shutdown (December 22, 2003 – March 17 for ISAC beam production), and a fall mini shutdown (September 13 – October 6).

The major jobs completed for ISAC included: rf system maintenance (coated surfaces of bunch rotator with Aquadag, commissioned spare control boards, design modifications for DTL #1 cooling system, commissioned remote controls for DTL #5 amp), implementation of access control system for electrical services room and DRAGON, OLIS work (MRO, source commissioning, controls MRO).

Completed target hall work included: ITW module access area MRO (rerouted cabling, cooling and vacuum services to tidy up the original installation), ITE

(EX1 harp MRO), TM1 work (replace target at ITW, replace faulty connector with new wiring harness for steering magnet), laser ion source alignment at ITW, installed modified ECR on TM3 and ECR tests (without target) at ITE.

CONTRACT ADMINISTRATION

In the past year three contracts were awarded: Linde Kryotechnik Agisac of Switzerland supplied and commissioned the refrigerator system for Phase I of the ISAC-II linac. The ISAC-II cryogenic refrigeration system warm piping was supplied and installed by Lockerbie and Hole Contracting Limited of New Westminster, BC. The ISAC-II Phase I helium gas storage tank was purchased from Gary L. Nadon Enterprises of Vancouver, BC.

Personnel Resources

ISAC-I

In 2004 the average monthly personnel effort for ISAC-I decreased by approximately 1 person per month to an average of 42.20 FTE people per month (see Fig. 222). In 2003 the FTE effort per month was 43.28 people. The total work effort expended on ISAC-I from the start of the project January 1, 1996 to December 31, 2004 has been 559.01 years, based on a FTE work-month of 150 hours per person.

ISAC-II

The recording of work effort for ISAC-II started October 1, 2000 (see Fig. 223). The work effort was recorded as "Project Management and Administration" up until March 31, 2002. Commencing April 1, 2002 the work effort was monitored by section. In 2004 the average monthly personnel effort for ISAC-II increased by approximately 1.5 people per month to an average of 21.11 FTE people per month (see Fig. 223). In 2003 the FTE effort per month was 19.53 people. The total work effort expended on ISAC-II from the start of the project October 1, 2000 to December 31, 2004 has been 56.91 years, based on a FTE work-month of 150 hours per person. Figure 224 shows the FTE years of work effort for each section of ISAC-II since the project began.

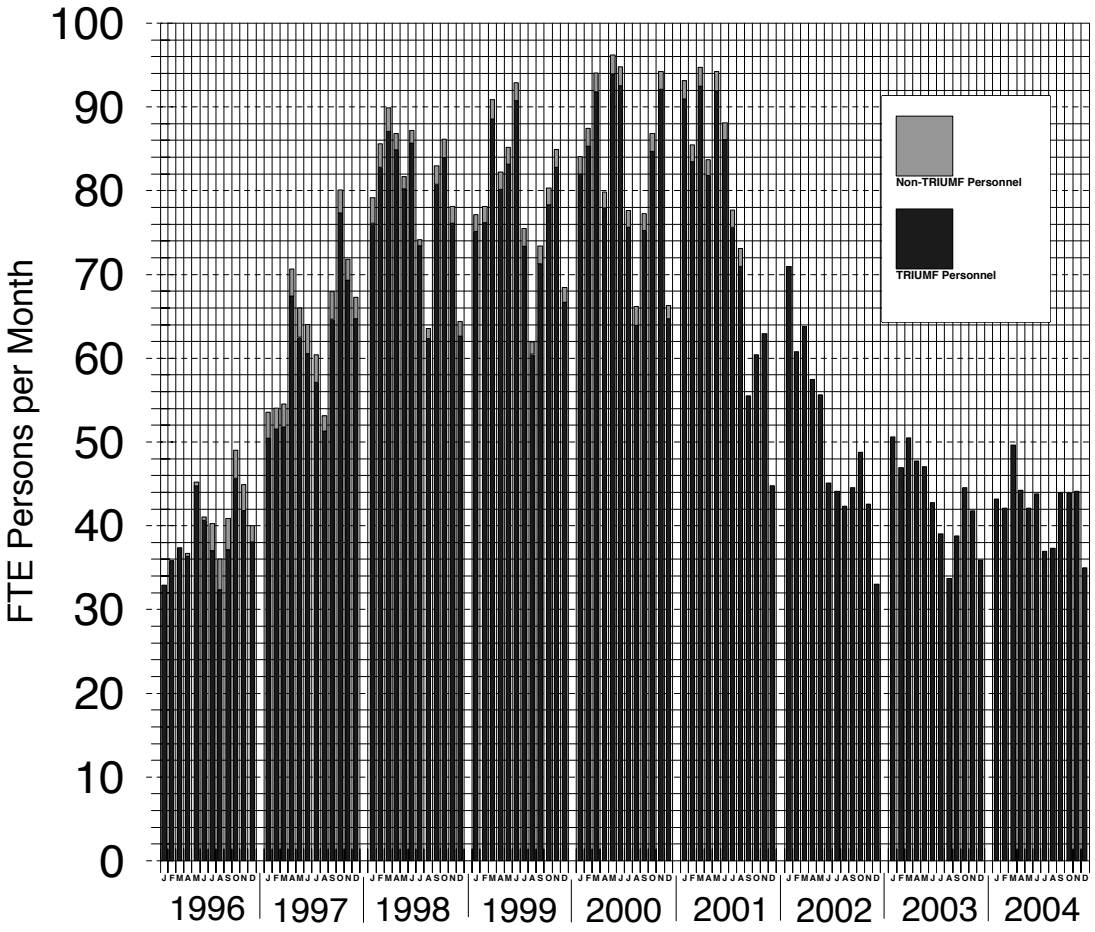

Fig. 222. ISAC-I monthly personnel effort, January 1, 1996 to December 31, 2004.

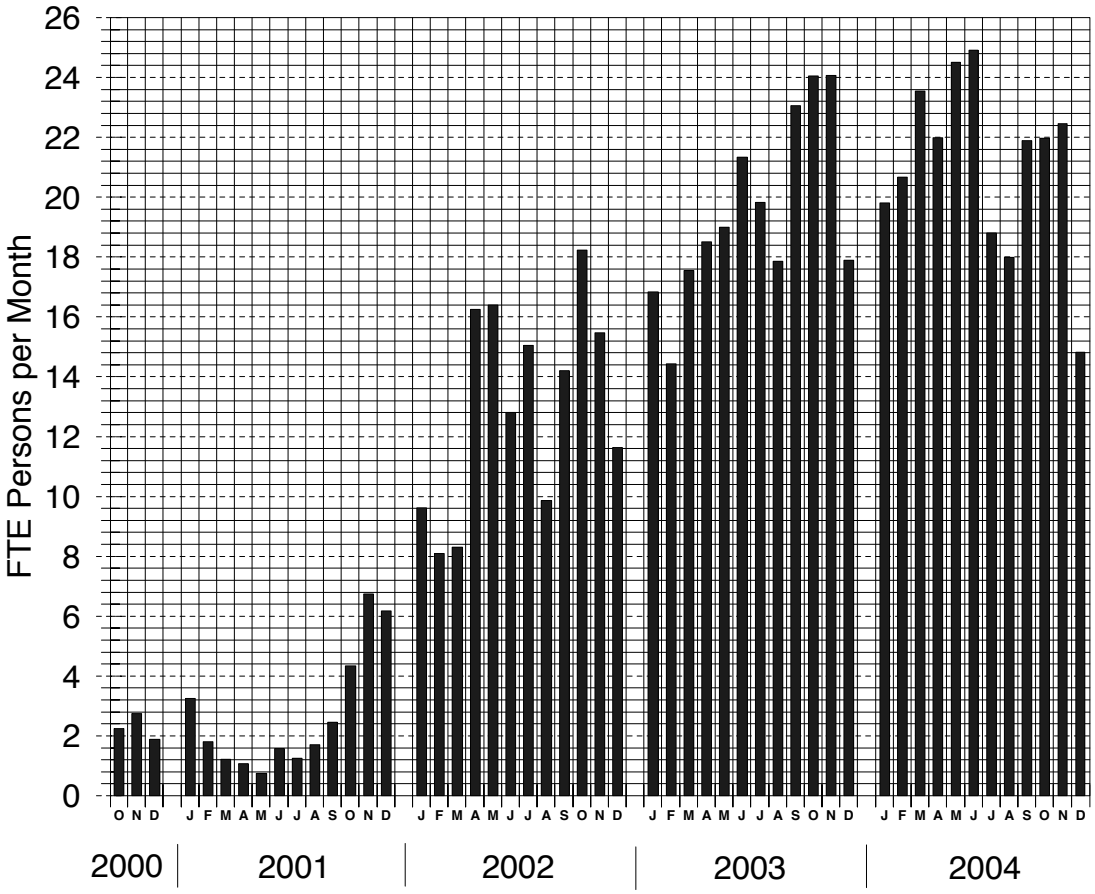

Fig. 223. ISAC-II monthly personnel effort, October 1, 2000 to December 31, 2004.

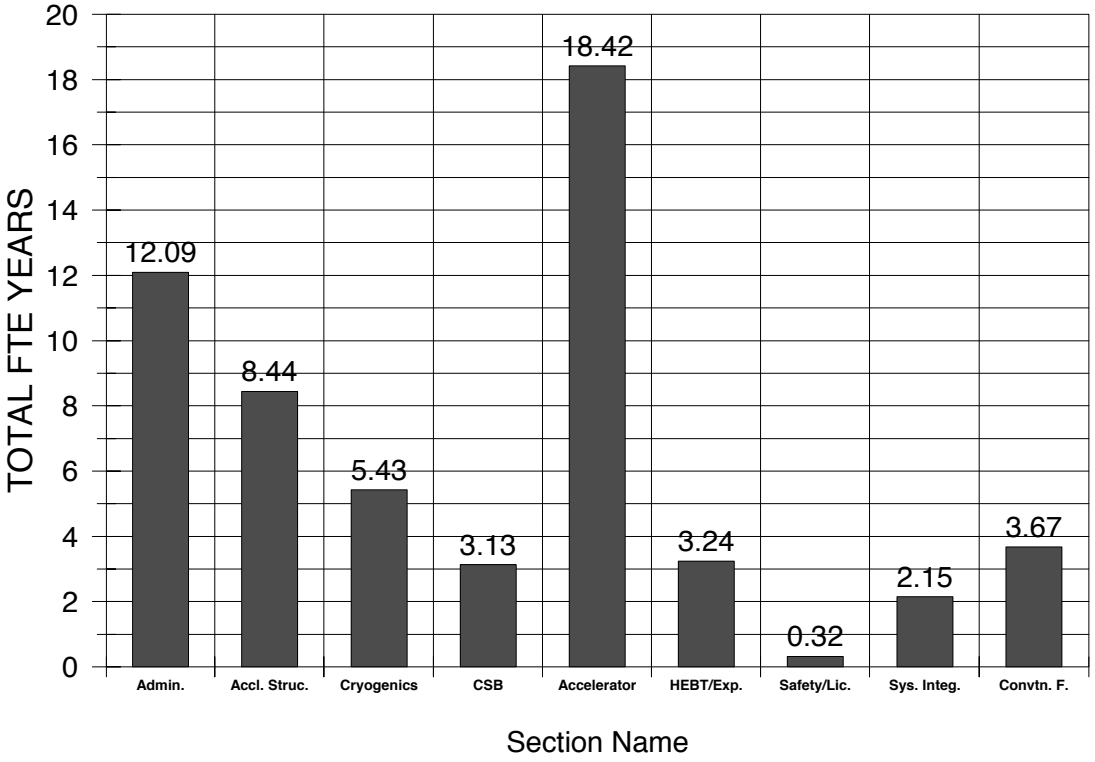

Fig. 224. ISAC-II total personnel effort, October 1, 2000 to December 31, 2004 shown by section.

ISAC-II CONVENTIONAL FACILITIES AND INFRASTRUCTURE

Activities in ISAC-II were mostly design and construction projects. In addition, we continued to provide engineering support to other groups and users and were involved in the preparation of specifications documents, and sat on several engineering review panels. Concurrently, civil construction deficiencies and warranty repairs continued, with the exception of the vault door deficiency. TRIUMF has taken this project into its own hands since the contractor was unwilling to properly fix the problem. We are currently reviewing the design concept, which includes using Thompson rollers instead of Hillman rollers.

On the mechanical services front, the depleted oxygen sensor system went through the entire process of design, review, tendering and construction. It was started up successfully just before Christmas, however, a few minor deficiencies remained and will be addressed during the winter shutdown. Air conditioning to the network computing centre continues to be scrutinized as it appears the thermal cycling provided by these units may not be sufficient for the sensitive electronics, in particular disk drives. There is some indication that temperature fluctuations greater than 1°C/3 min affect the performance and increase the failure rate of these devices. A solution is being studied. Several large mechanical projects came to an end. The NALCW system was started up and provided water to its first consumer, the rf test stand. Because of the contamination of the mains during construction of ISAC-II, cleaning and repeated flushing was required before water could be allowed to return to ISAC-I. After water was allowed to flow, the return water to ISAC-I was filtered for several weeks to ensure all loose materials were captured. One casualty was the de-ionizing resin which faithfully polished the new piping system before expiring. After having to polish the ISAC-I piping and five more years of service it was near the end anyway. A major upgrade of the air exhaust in the helium compressor room was also completed. The existing system was not able to meet the 40,000 CFM required.

On the electrical services front, we record the successful completion of the services for the helium refrigeration system, which was commissioned during the winter shutdown and the installation of the S-bend beam transport services. Activities in the latter will continue well into next spring, with commissioning expected in early June, 2005. Other activities to report include: the installation of a crane for the rf test area on the NW side of the experimental hall; a study to determine whether the services for the CSB would fit into the service room next to the mass separator vault in ISAC-I; the design of the upgrade of the UPS power distribution for the network computer system and the expansion of the UPS distribution to supply the liquefier room and the S-bend. The review of the electrical power needs of the ISAC facility was also completed. It pointed to a few significant upgrades and re-alignments of the main power distribution centres to accommodate future load growth. The first of these upgrades, the MCC-S, will start during this coming winter shutdown with the remainder to follow over the next couple of years. Redundant fibre links were installed between ISAC-II and the administration building. These included 6 strands of single-mode fibres, and 48 strands of multi-fibres (24 of which are spares). DATA cabling was completed for room 163, the rf services and S-bend, room 164, the liquefier room, room 166, the helium compressor room, the vault and the experimental hall. The power supply room DATA cabling is planned for next year.

ISAC-II ACCELERATORS

Introduction

The ISAC-II linac is being installed in stages. The superconducting linac is composed of two-gap, bulk niobium, quarter wave rf cavities, for acceleration, and superconducting solenoids, for periodic transverse focusing, housed in several cryomodules. The initial stage to be completed in 2005 includes the installation of a transfer line from the ISAC DTL ($E = 1.5\,\mathrm{MeV/u}$) and twenty medium beta cavities in five cryomodules to produce 20 MV of accelerating voltage for initial experiments.

Cavity Testing

To date, fifteen cavities have been characterized via cold tests. Typical treatment involves a 30–40 minute high pressure water rinse and 24 hour air dry in a clean room, followed by vacuum pumping and bakeout at 95°C for 48 hours, then an LN_2 pre-cool to 160 K over 48 hours followed by helium transfer and test. A distribution of the cavity performance is shown in Fig. 225 for both the characteristic fields at 7 W cavity power and at maximum power. Four cavities out of the fifteen have not met specification with one cavity limited to 3 MV/m. Developments are under way to determine the cause of the reduced performance. A further chemical polishing may be required.

Medium Beta Cryomodule

The vacuum tank consists of a stainless steel rectangular box and lid. All services and feedthroughs are located on the lid. The entire cold mass is surrounded by a forced flow, liquid nitrogen cooled, copper thermal shield. A μ-metal magnetic shield, consisting of 1 mm Conetic panels is attached to the inside of the vacuum tank outside the LN_2 shield. A single LN_2 panel and

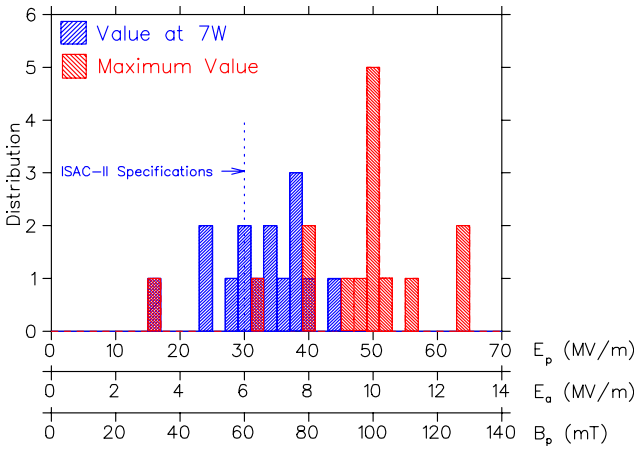

Fig. 225. Histogram summarizing cavity performance for fifteen tested cavities. Shown are the numbers of cavities achieving a certain gradient at 7 W helium load (blue) and the numbers of cavities achieving a certain maximum field (red).

μ-metal shield suspended from the lid make up the top thermal and magnetic enclosure respectively. The μ metal is designed to suppress the ambient field by a factor of twenty. Cavities and solenoids are suspended from a common support frame itself suspended from the tank lid (Fig. 226). Each cryomodule has a single vacuum system for thermo-isolation and beam acceleration. The cavities must be aligned to within 0.4 mm and the solenoid to 0.2 mm. A wire position monitor system has been developed to monitor the position of the cold mass during thermal cycling.

The ISAC-II medium beta cavity design goal is to operate up to 6 MV/m across an 18 cm effective length with $P_{\rm cav} \leq 7$ W. The gradient corresponds to an acceleration voltage of 1.1 MV, a challenging

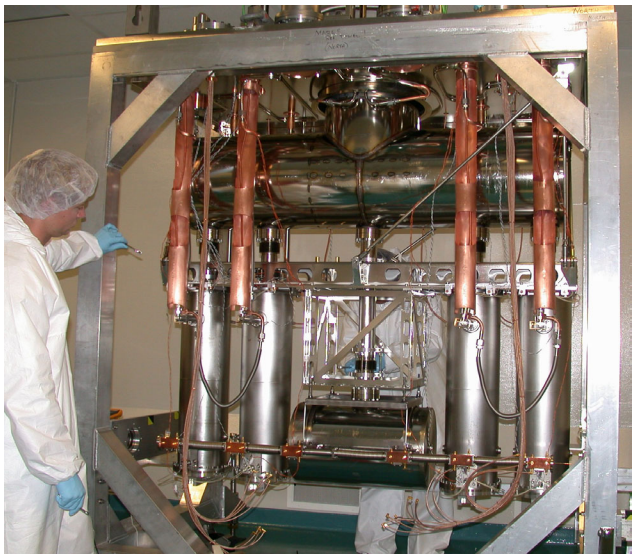

Fig. 226. Cryomodule top assembly in the assembly frame prior to the cold test.

peak surface field of $E_p = 30$ MV/m and a stored energy of $U_o = 3.2$ J and is a significant increase over other operating heavy ion facilities. To achieve stable phase and amplitude control, the cavity natural bandwidth of ± 0.1 Hz is broadened by overcoupling to accommodate detuning by microphonic noise and helium pressure fluctuation. The chosen tuning bandwidth of ± 20 Hz demands a cw forward power of $\sim$200 W ($\beta \simeq 200$) and peak power capability of $\sim$400 W to be delivered to the coupling loop. A new coupler has been developed that reduces the helium load to less than 0.5 W at $P_f = 200$ W. The tuning plate on the bottom of the cavity is actuated by a vertically mounted permanent magnet linear servo motor at the top of the cryostat using a "zero backlash" lever and push rod configuration through a bellows feed-through. The system resolution at the tuner plate centre is $\sim$0.055 μm (0.3 Hz). The solenoids are equiped with bucking coils to reduce the fringe field in the adjacent cavities to $<$50 mT.

Cryomodule Testing

The cryomodule assembly and commissioning tests are conducted in the clean laboratory area in the new ISAC-II building. Three cold tests have been completed. An EPICS based control interface is used to interact remotely with the cryomodule systems during the test.

An initial cold test I in April, without rf ancillaries installed, characterized cryogenic performance and determined the warm off-set required to achieve cold alignment. In cold test II the integrity of the rf and solenoid systems was checked as well as the repeatability of the intial cold alignment. In cold test III the cavities were prepared for final installation with a final high pressure water rinse before reassembly with machined alignment shims. During this third test the cryomodule was outfitted with an alpha source and acceleration was demonstrated for the first time.

Alignment

The position of the cold mass as monitored by the WPM at three cold LN_2 temperatures is repeatable to within ± 50 μm vertically and ± 100 μm horizontally. Due to the different materials involved, the solenoid experiences more vertical contraction, with 4.4 mm at LN_2 and 5 mm at LHe temperatures while the cavities contract 3.3 mm at LN_2 and 3.8 mm at LHe temperatures. For beam dynamics reasons we require the cavity beamport centre line to be 0.75 mm below the beam centre line as defined by the solenoid. Cold tests I and II results show that final alignment is achieved by aligning the cavities while warm to (0,0,0,0) horizontally and (+0.28,+0.38,+0.38,+0.28) vertically with the solenoid at $(x, y) = (0, 0)$. Optical targets are then

placed in the upstream and downstream solenoid bore for cold test III. The beam axis is defined by optical targets on the beam aperture of the tank. Adjusters located on the lid are used to align the solenoid targets to the beam axis targets after cooling the cold mass.

Cryogenics

The helium transfer line fits to a manifold in the helium space that delivers helium in parallel to a series of 3 mm tubes that are routed to the bottom of each of the cold mass elements. This system works well to efficiently cool the cryomodule. At a total flow of 75 l/hr the cavities cool together at a rate of 100 K/hr while the solenoid cools at a rate of 20 K/hr due to its larger mass. The static load on the helium in the three tests is measured to be 11 W, 16 W and 13 W respectively. The differences are due to the variations in the internal cabling and equipment used in each test. The final value of 13 W is representative of the load for the on-line system and compares well to estimates during the design phase. The LN_2 flow required to keep the side shield less than 100 K is ∼5 l/hr, matching design estimates.

Cavities and solenoid

The cavities are first baked at ∼90°C for 24 hours. The cold mass is pre-cooled with LN_2 to about 200 K before helium transfer. The quality factor of each cavity is determined by measuring the time constant of the field decay in pulsed mode at critical coupling. The Q_0 values for test II, presented in Table XLVI, are similar to those measured in the single cavity cryostat indicating that the μ-metal reduces the remnant magnetic field to a sufficient level. In the first rf test (cold test II) the solenoid is ramped up to 9 T with cavities 2 and 3 ON. The cavities remain ON and the measured Q_0 values do not change. The solenoid and cavities are then warmed above transition. After a subsequent cooldown the cavity Q_0 values are again measured. There is no change in the values showing that fields induced by the solenoid in the region of the cavities are tolerably small.

After test I the cold mass is removed from the cryomodule and the top plate is replaced by sheets of μ metal. The remnant field inside measured longitudinally at the beam axis and vertically in the cryomodule (−1 is at the top) are shown in Fig. 227. Also plotted are values from new cryomodule SCB1 after assembly and before powering the solenoid. Note that the fields in SCB3 are significantly higher especially in the middle of the cryomodule in close proximity to the solenoid. It appears that the solenoid is magnetizing the μ metal enclosure or the nickel in the LN_2 shield. In subsequent tests a hysteresis cycling of the cryomodule will be employed to reduce the remnant field. A field higher than 5 μT will start affecting the performance.

Table XLVI. Cavity performance during cold tests II and III.

Test	Cavity 1 $Q/10^9$	Cavity 2 $Q/10^9$	Cavity 3 $Q/10^9$	Cavity 4 $Q/10^9$
II	1.5	1.4	1.5	1.3
III-1	1.25	1.03	1.42	1.13
III-2	0.745	0.89	1.17	0.76
III-3	0.41	0.20	0.19	0.28
III-4	1.12	0.76	1.18	0.75

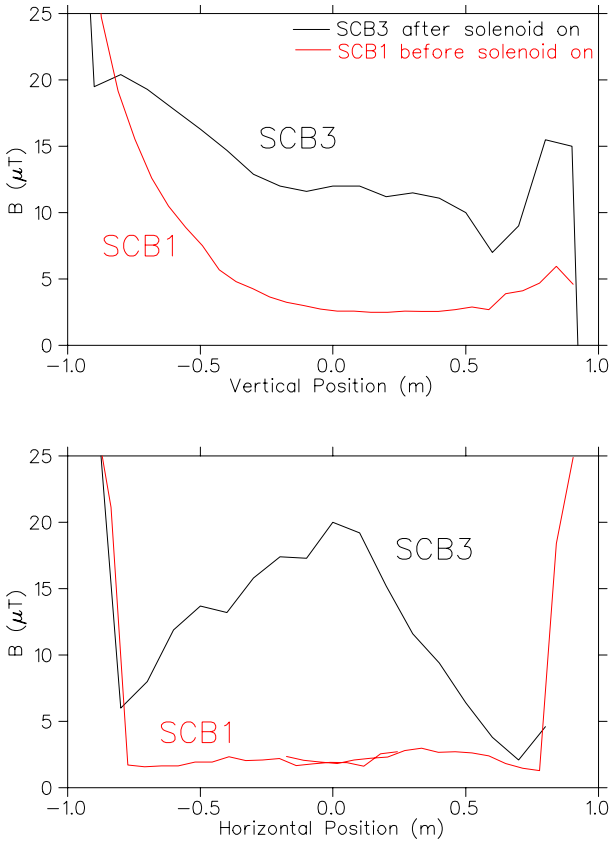

Fig. 227. Longitudinal and vertical magnetic field maps inside cryomodule SCB3 (warm) after test II compared to a mapping on new cryomodule SCB1.

In test II Q_0 values are taken periodically and the results are reported in Table XLVI. We attribute the large range in values to trapped flux in the solenoid. Since the modules are filled from dewars the cryomodules are allowed to warm overnight. Fig. 228 gives the temperature of the solenoid and cavities during the test. Labels Q1–Q4 indicate the time of Q measurements corresponding to III-1 to III-4 in Table XLVI. Labels S1–S5 indicate powering of the solenoid. The cavity temperatures rise above transition during the night but portions of the solenoid remain below transition. In addition for cases S1, S4 and S5 a hysteresis cycling of the solenoid occurs. For cases S2 and S3 no

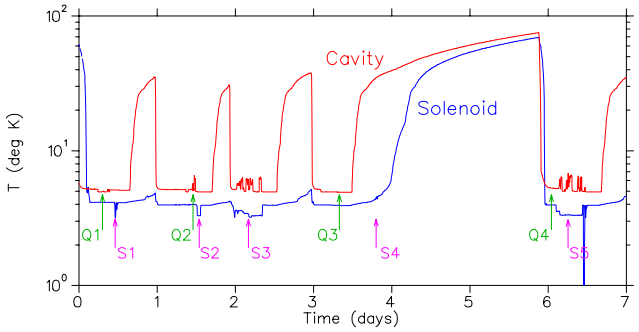

Fig. 228. Temperature history of cavities and solenoid during test III. Q1–Q4 indicate the time of the Q_0 measurements reported in Table XLVI and S1–S5 indicate solenoid on periods.

cycling is done. Taking the Q_0 values for case III-1 as a base and assuming the subsequent reduction in Q_0 is due to an increase in $R_{\rm mag}$ gives an estimate of the magnetic field increase. The resulting estimations are summarized in Fig. 229. Note that the field increase is largest near the solenoid.

RF control and tuning

A new EPICS GUI interface provided remote tuning control for the four cavities during test III. All four cavities were locked at ISAC-II specifications, $f = 106.08$ MHz, $E_a = 6$ MV/m with a coupling $\beta \simeq 200$ for tuning bandwidth. Stable operation was maintained for several hours. Tuner operation is tested by forcing pressure variations in the helium space. The tuner plate position of the four cavities during one perturbation cycle is shown in Fig. 230.

Alpha Acceleration

The cold tests establish the integrity of the cryomodule and rf ancillaries but do not qualify the unit as an accelerator. An off-line acceleration test with alpha particles from a radioactive source has several key motivations: to establish the integrity of the cryomodule as an accelerator months before an on-line beam

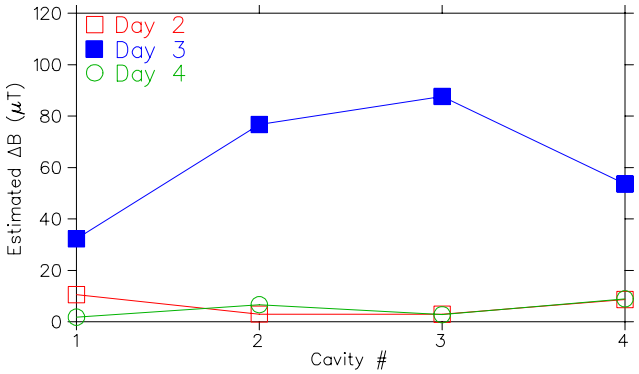

Fig. 229. Estimated change in background magnetic field at times corresponding to Q2–Q4 compared to field at Q1.

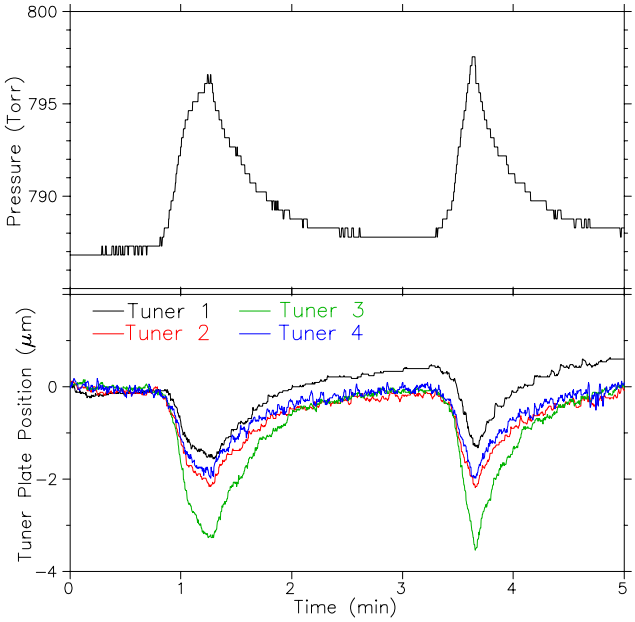

Fig. 230. Tuner position response for forced pressure fluctuations in the helium space. The cavity gradient is 6 MV/m with a bandwidth of ±20 Hz.

test is possible, to measure directly the total voltage of the cryomodule, and to gain first experience with the proposed ISAC-II accelerator control system and GUI interface.

Test set-up

The cryomodule tests are done in the test pit of the ISAC-II clean room. The source is installed in the beam aperture of the upstream diagnostic box and the silicon detector is mounted in a diagnostic box positioned at the exit of the cryomodule downstream of the isolation valve as shown in Fig. 231.

A ^{244}Cm alpha source, borrowed for the experiment, emits alpha particles with energies 5.76 MeV (24%) and 5.81 MeV (76%) with a half life of 18 years and an activity of 10^7 Bq. It is covered by a 5 μm foil of Ti to contain the radioactive material. Due to safety concerns over foil rupture and possible migration of

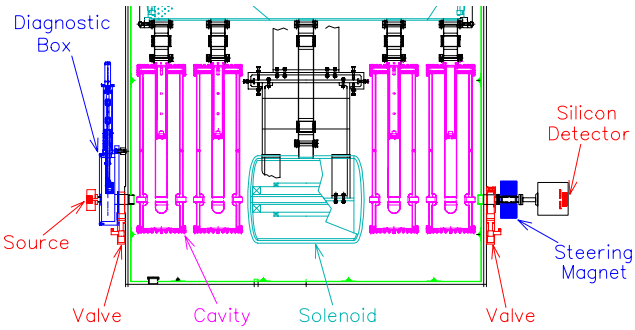

Fig. 231. The test set-up for the alpha particle acceleration. The particles are accelerated from left to right.

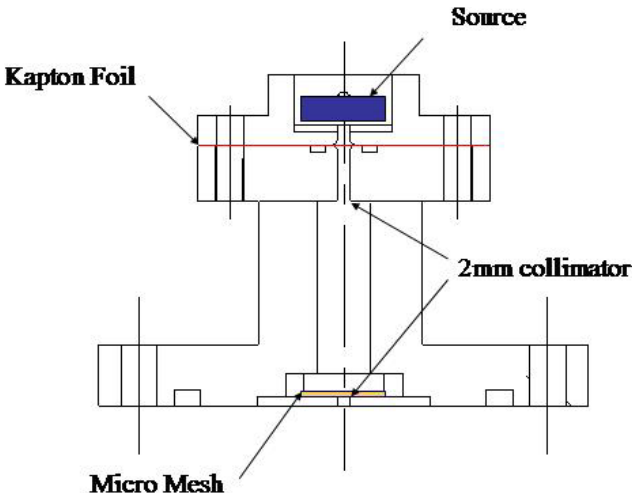

Fig. 232. The source and holder.

the alpha emitters the source remains at atmosphere. A source holder (Fig. 232) is equipped with an 8 μm kapton window over a 2 mm aperture that serves as a vacuum window. Another 2 mm aperture lies downstream to further collimate the alpha beam and limit the molecular conductance in case of window failure. A foil micro-mesh (60% transmission) is installed in the downstream 2 mm aperture to catch foil fragments in the case of window rupture. The source holder has a vacuum flange on the downstream end that mates with the upstream diagnostic box of the cryomodule. The Ti and kapton foils degrade the energy spectrum of the alphas to 2.85 MeV with a standard deviation of 200 keV.

A diagnostic box is placed 40 cm downstream of the cryomodule and is connected to the vacuum space by a 5 cm diameter vacuum pipe that can be isolated by a VAT valve connected to the module. A steering magnet is placed between the cryomodule and the diagnostic box to clear any electrons accelerated by the cavities. A silicon surface barrier detector is mounted on the back of the box with a moveable collimator wheel assembly in front to intercept the deflected electrons.

An accelerating gradient of 6 MV/m corresponds to a peak voltage gain of 1.08 MV for an effective length of 18 cm. The alpha particle average initial energy of 2.85 MeV/u ($\beta = 3.9\%$) is low with respect to the design geometry of the cavity. The expected transit time factors, energy gain/cavity and expected final energy are given in Table XLVII.

Multi-particle simulations are done with the linac code LANA. The source collimator geometry is modelled to generate a realistic initial transverse phase space. The transverse beam parameters after collimation are $\alpha_{x,y} = -1.0$, $\beta_{x,y} = 0.0055$ mm-mrad and $\beta\epsilon_{x,y} = 0.45\ \pi$ mm-mrad. Realistic three-dimensional fields generated by HFSS are used to represent the

Table XLVII. Expected energy gain for 2.85 MeV alpha particles accelerated through four ISAC-II cavities at 6 MV/m.

Cavity	$E_{\rm in}$	T/T_0	ΔE (MeV)	$E_{\rm out}$
1	2.85	0.46	0.99	3.84
2	3.84	0.75	1.62	5.46
3	5.46	0.92	1.99	7.45
4	7.45	0.99	2.14	9.59

cavities and the solenoid is modelled with the standard linear matrix. Previous modelling studies have shown that the solenoid matrix represents a ray traced solution to close approximation.

Test results

The collimation reduces the intensity to ∼40 pps while the accelerator acceptance reduces this further to ∼4 pps. Since the beam is unbunched, the actual count distribution for the higher energy particles of interest is very weak. The cavities are turned on sequentially starting at the upstream end. Each cavity is first set to the correct voltage. The solenoid is set to the optimal value found from the simulations. With the exception of cavity 1, the cavity phase is scanned in 30° phase increments to find the optimum phase. Each phase set point takes 5–10 minutes before a reasonable spectra is obtained. Once the correct phase is determined, the spectra for the optimized settings are taken for twenty minutes.

The spectrum for the cavities off as well as the four spectra as the cavities are turned on sequentially are plotted in Fig. 233. Maximum particle energies for the four cases are 4.2, 5.8, 7.4 and 9.4 MeV. The results for the first two cavities are higher than the calculated single particle values in Table XLVII due to the large energy spread in the initial beam. The maximum final energy depends on the phasing of the cavities and the relationship of the cavity phases to the initial energy of the beam. During the test, cavity phases are chosen to optimize the energy of a statistically significant number of particles. These particles would come from some energy band located between the mean initial energy and the highest initial energy.

A true analysis of the cavity voltage can only be done with a simulation. Due to the poor quality of the injected beam, most of the ions are only partially accelerated. The spectra for the unbunched, uncollimated beam provide, however, a spectral fingerprint. As the voltage and phase of the cavities in simulation are varied the distribution of the most energetic ions, as well as that of the lower energy peaks, shifts and an unambiguous fit of cavity voltage is possible. The best fit simulations are superimposed on the test data in Fig. 233. The corresponding

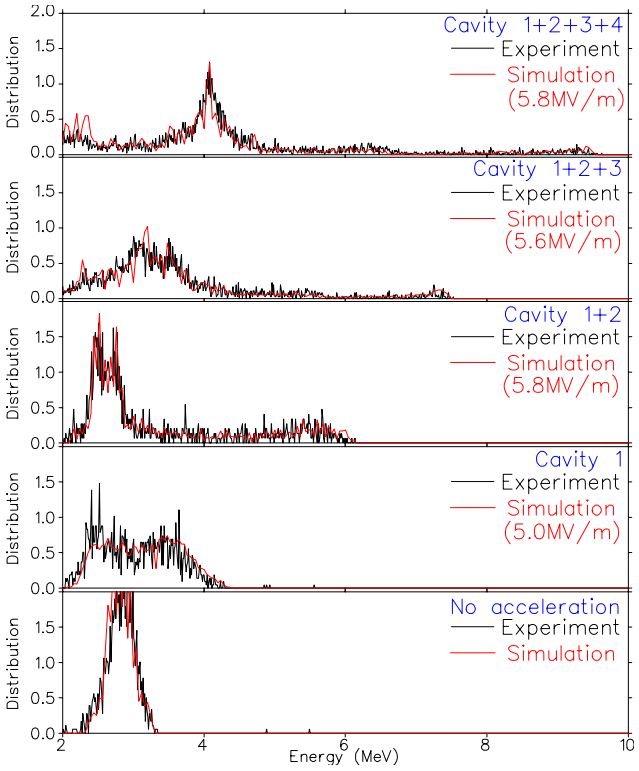

Fig. 233. Experimental spectra (black) and simulation result (red) for no acceleration, and for each case with cavities from 1 to 4 on sequentially at the nominal voltage of 6 MV/m.

cavity voltages for these cases are 5, 5.8, 5.6, and 5.8 MV/m for cavities 1 through 4 respectively for an average gradient of 5.6.

High Beta Cavities

The linac for ISAC-II comprises twenty cavities of medium β quarter wave cavities now in the installation phase. A second stage will see the installation of ∼20 MV of high β quarter wave cavities. The cavity structure choice depends on the efficiency of operation, cost, stability, beam dynamics and schedule. Three cavity variants are considered and shown in Fig. 234. The benchmark cavity, (a) *round141*, has identical transverse dimensions to the medium beta cavity but is designed as a 141 MHz cavity by shortening the overall length and adjusting the gap. In a second variant,

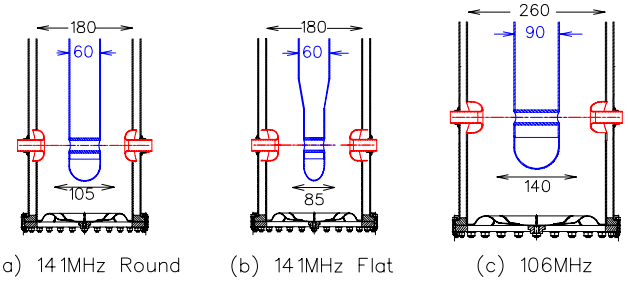

Fig. 234. Three cavity variants considered in the study.

(c) *round106*, the cavity frequency is kept at 106 MHz but the cavity transverse dimensions are scaled to increase the beta from 7.1% to 10.4%. The quadrupole asymmetry in the accelerating fields is somewhat larger in the high frequency case by virtue of the smaller inner conductor. A third variant, (b) *flat141*, is also considered where the 141 MHz cavity inner conductor is flattened near the beam ports to produce a smaller quadrupole asymmetry. This variant has a lower optimum beta, 9%, suitable for use in the beginning of the high beta section.

Previous beam dynamics studies have shown that the reduced quadrupole asymmetry in the *round106* cavity results in less asymmetry in the transverse envelope compared to the other two 141 MHz variants. However, the transverse and longitudinal emittance growth for the three cases are virtually identical. The beam centroid shifts are tolerably small in all cases.

RF characteristics

The rf parameters of the three cavity variants are given in Table XLVIII. The cavity rf properties are simulated in HFSS. We compare all cavities at a gradient of 6 MV/m calculated over the cavity length defined as the inside diameter of the outer rf surface. There is little difference between the two 141 MHz variants except for the higher peak surface field in the *flat141* variant. Instead we concentrate here on the comparison of the *round141* and the *round106* variants. Due to the increased voltage the main practical difference is that fewer sub-systems (14 as compared to 20) would be required for the lower frequency. However, due to the higher stored energy and somewhat higher Q_0 (see

Table XLVIII. Parameters of cavity variants.

Parameter	*round141*	*flat141*	*round106*
f (MHz)	141.4	141.4	106.1
β_0	0.104	0.09	0.103
TTF_0	0.089	0.086	0.093
Bore (mm)	20	20	20
Gap (mm)	45	45	50
Drift tube (mm)	60	40	90
$L_{\rm eff}$ (mm)	180	180	260
Height (mm)	577	577	737
Δy (mm)	1.3	1.0	2.0
$f_{\rm mech}$ (Hz)	150	150	134
E_a (MV/m)	6	6	6
V (MV) @ 6 MV/m	1.08	1.08	1.56
E_p/E_a	4.7	5.6	4.6
B_p/E_a (mT/MV/m)	10.3	10.5	9.9
U/E_a^2 (J/(MV/m)^2)	0.073	0.078	0.194
R_sQ_0 (Ω)	24.8	24.9	26.8
R_{sh}/Q (Ω)	499	470	521

below) more power is required to provide a sufficient tuning bandwidth.

Let us examine the role of rf frequency in cavity scaling. The surface resistance is given by

$$R_s = R_{BCS} + R_{\rm mag} + R_0$$

where

$$R_{BCS} = 2 \times 10^{-4} \frac{1}{T} (\frac{f}{1.5})^2 e^{-17.7/T}$$

and

$$R_{\rm mag} = 0.3 n\Omega \cdot H_{\rm ext}(mOe) \sqrt{f(GHz)}\,.$$

Results of these expressions are shown in Table XLIX assuming a magnetic field attenuation factor of five from the earth's field. The TRIUMF medium beta cavity has a typical Q of 1.5×10^9 at low field that droops to 5×10^8 at a gradient of 6 MV/m. Since $R_s Q = 19\ \Omega$ for this cavity, this corresponds to surface resistance values of 12.7 and 38.2 nΩ. Assuming R_0 is independent of frequency we can estimate that the high-field surface resistance for the 141 MHz cavity is enhanced due to the increased values of R_{BCS} and $R_{\rm mag}$ to be 42.5 nΩ, an increase of 11%. Using these values of R_s and the tablulated values of $R_s Q_o$ gives expected Q_0 values of 5.8×10^8 and 7×10^8 respectively for the *round141* and *round106* cavity respectively. The cavity power dissipation, $P_{\rm cav} = \omega_o U/Q_0$, is listed in Table XLIX.

The increased quality factor of the 106 MHz cavity increases the amount of overcoupling required to achieve a specified rf bandwidth (in our case $\Delta f/f = 4 \times 10^{-7}$). The forward power can be calculated from the coupling factor, β, and the cavity power using $P_f = P_{\rm cav} * (\beta+1)^2/(4\beta)$. To provide for the bandwidth the peak amplifier power must be sufficient to deliver twice the required forward power after considering the line losses. These deliberations lead us to estimate that the required amplifier would be almost a factor of two larger in the 106 MHz case.

Table XLIX. Frequency dependence of surface resistance and cavity power.

Parameter	106 MHz	141 MHz
R_{BCS} (nΩ)	3.5	6.3
$R_{\rm mag}$ (nΩ)	9.8	11.3
R_0 (nΩ)	25	25
R_s (nΩ)	38.2	42.5
Q_0 @ 6 MV/m	7×10^8	5.8×10^8
$P_{\rm cav}$ (W) @ 6 MV/m	6.7	4.2
β	280	230
$P_{\rm amp}$ (W) @ 6 MV/m	1200	620

Cavity choice

There is no strong beam dynamics argument to choose one variant over another. The total dissipated cavity power is 17% less in the high frequency cavity and the total amplifier power is 29% less. The high frequency cavity is also somewhat more mechanically stable. These advantages are not sufficient to force a cavity choice. The most compelling argument is that the design time for the 141 MHz cavity, the ancillaries and the cryomodule will be significantly less. This is balanced somewhat by the attractiveness of reducing the number of sub-systems by adopting the lower frequency. However, the 141 MHz option has been chosen as the high beta cavity for ISAC-II.

Cryogenics

The ISAC-II Phase I cryogenic system was specified for tender in early 2003. Initially a complete turnkey system including refrigerator, warm and cold piping, buffer tank, helium dewar, compressors, gas management and oil removal system was requested. All returning bids were overbudget. TRIUMF decided to take on a larger role in the project in order to reduce the capital costs. The scope of the initial contract was restricted to the major refrigerator components: refrigerator, main and recovery compressor and ORS/gas management. TRIUMF assumed the responsibility for installation of the Linde refrigerator components as well as the management of the contract for the installation of the warm piping by a local installer. In addition TRIUMF acquired and installed the buffer tank and helium dewar. The cold distribution is now specified by TRIUMF and the contract for manufacture and installation will be awarded in 2005.

In the first phase, to be completed by December, 2005, five medium beta cryomodules will be installed. The linac cryomodules will be cooled by 4.5 K LHe at 1.4 bar. The measured static heat load for a single cryomodule is 13 W with a LN_2 feed of 6 l/hr. Together with estimated thermal losses from the cold distribution of 72 W this gives a total static load of 137 W. The budget for active load component is 8 W per cavity giving 160 W for the twenty medium beta cavities for a total estimated heat load of 297 W. A TC50 cold box complete with oil removal and gas management system, main and recovery compressors was purchased from Linde and installed by TRIUMF with commissioning slated for early 2005.

Cold distribution

The refrigerator supplies liquid helium to a dewar via a Linde supplied transfer line. The main trunk supply line is fed LHe from the dewar. The cryomodules are fed in parallel from a helium supply trunk line through variable supply valves and field joints. The

cold return from the cryomodules comes back to the trunk cold return line through open/close valves and field joints. During cooldown, when warmer than 20 K, the returning gas is sent back to the suction side of the compressor through the warm return piping. Keep cold sections with proportional valves are required at the end of the trunk lines to join the trunk supply and the trunk cold return. Future expansion will involve demounting the keep cold sections, extending the trunk and cryomodule feed lines and remounting the keep cold sections. A second refrigerator will be added in two years. Pipe sizes and expected mass flows for the cold distribution are given in Table L. Valves specified for the middle of the two trunk lines are for future installations to divide flows between two refrigerators. They can be installed as just valve seats with the stems left out, and run continuously open for Phase I. In addition to the branch lines supplying the five cryomodules, a secondary line off the main trunk supply is required to deliver LHe to the ISAC-II test/assembly area. All supply and cold return piping is vacuum jacketed and, except for the short cryomodule feed lines, is cooled with LN_2.

A cross section of vault and refrigerator room is shown in Fig. 235.

Table L. Cold distribution specifications.

Pipe	Supply ID (mm)	Return ID (mm)	Mass flow (gm/s)
Dewar to trunk	18	45	25
Trunk	18	45	25
Cryomodule	13.8	32	5
Clean room	13.8	32	5
Keep cold	–	13.8	2

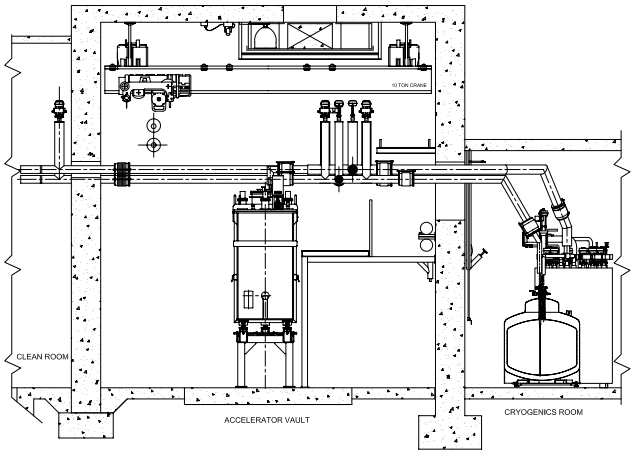

Fig. 235. Vault and refrigerator room cross section showing cryomodule, cold piping, service platform, helium dewar and cold box.

Beam Lines

The S-bend transport line from the ISAC-I hall to the superconducting linac is almost complete. The line consists of two achromatic bend sections of ∼120° with two 4Q straight segments between. A 35 MHz buncher between straight segments matches the beam from the ISAC-I DTL to injection into the SC linac.

The high energy beam line is designed with a removeable section to be compatible with the installation of the high beta cryomodules. This represents a full length of 8.84 m so two 4.42 m long 4Q sections are used. This periodicity is maintained to the end of the vault within all five 4Q sections. The sections can be tuned to unit cells with double focus points at the end of each section or to periodic doublet sections with a phase advance of ∼90° for multicharge transport. Previous studies have shown that the accelerator can accommodate multicharge beams up to $\Delta Q/Q = \pm 10\%$. The present beam line design will accommodate such beams with some emittance growth due to the mismatch at the first cell after the linac.

At present the plan is to use existing dipoles from Chalk River to deliver beam up to three experimental stations. The installation of these beam lines will be staged over the next several years.

ISAC-II HEBT AND EXPERIMENTAL HALL

The ISAC-II accelerator will take the beam from the DTL-1. To increase the mass range from 30 u to 150 u, we will rely on a charge state booster. Consequently, the expected beam emittance is larger than the one used for the DTL-1. Figure 236 shows the beam emittance as a function of the output beam energy. The solid curve is the nominal beam emittance, the dotted line represents the expected beam emittance if the charge state booster is in use. We have to assume the largest expected emittance in order to make sure that the transport calculations are realistic.

The design of the beam lines is based on the available magnets and quadrupoles from the Chalk River Laboratory. We have two Y-magnets and 18 magnetic quadrupoles that can be used for the ISAC-II beam lines.

Figure 237 shows the layout of the ISAC-II experimental area. The beam lines will be built in stages. For the moment, four facilities that we know about are to be installed in the ISAC-II experimental hall:

1. TIGRESS, a gamma ray spectrometer;
2. HERACLES, a heavy ion detector array for the study of reaction mechanisms;
3. A large acceptance light ion detector array for (p, p), (α, p), ... reactions; and
4. EMMA, a recoil spectrometer.

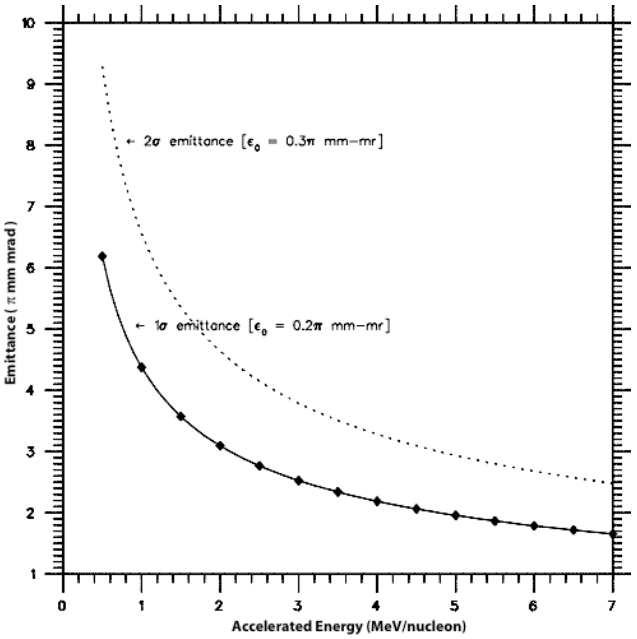

Fig. 236. Plot of the expected emittance as a function of the output energy.

Phase 0 in April, 2006 will accommodate a short beam line to perform the first beam experiment. It will most likely be a ^{21}Na Coulomb excitation experiment, which requires very little infrastructure.

Phase I (represented in light blue) will accommodate the TIGRESS facility with the beam dump. It will be completed during the fall, 2006.

Phase II is represented in red. Once the second leg is installed, we will be able to accommodate the HERACLES detector (light green), the TUDA-II detector facility, and the EMMA recoil spectrometer. The next step will be an expansion with a linear rail system which will allow TIGRESS to move from its stand-alone station to EMMA.

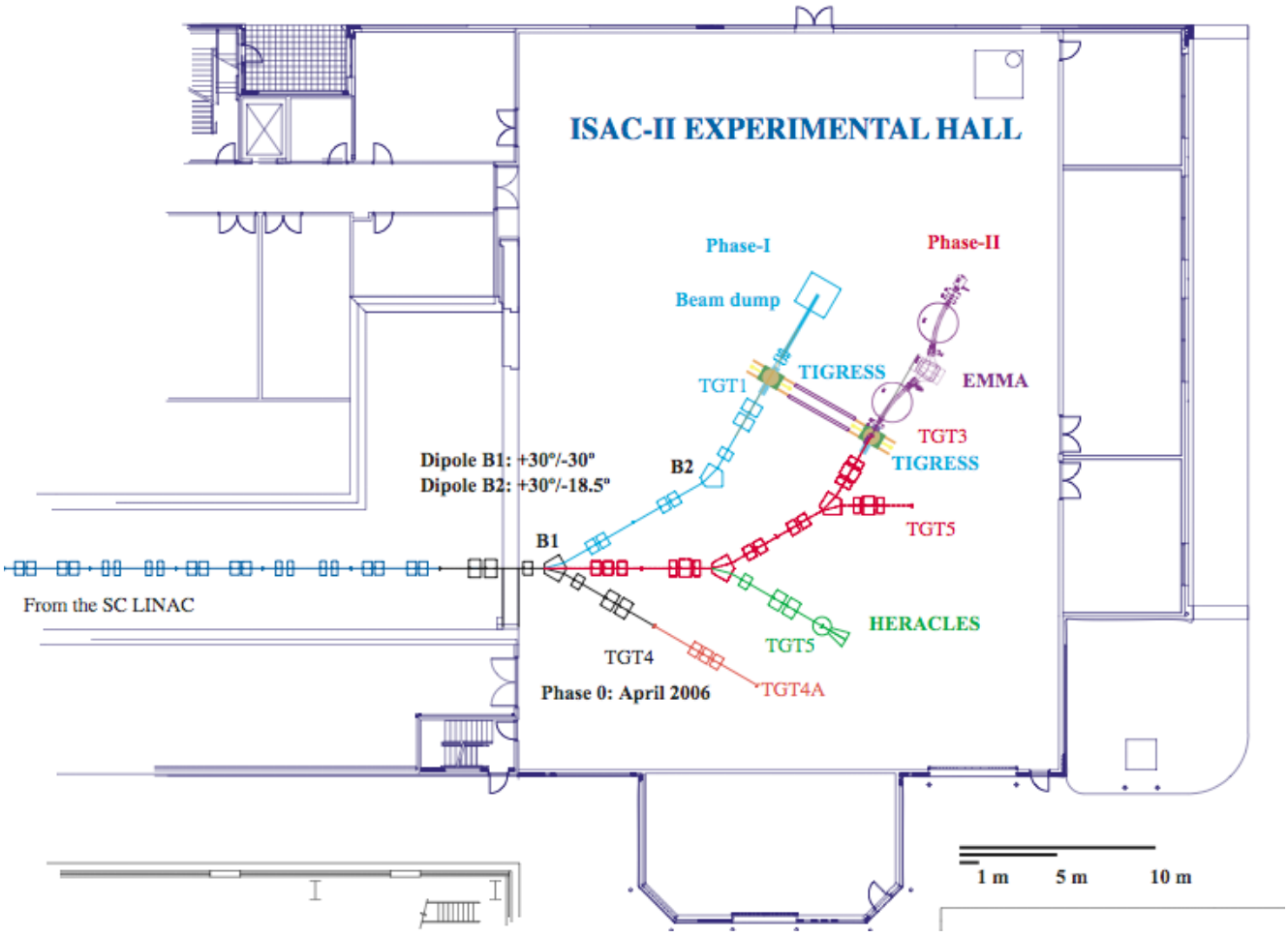

Fig. 237. Layout of the proposed beam lines for the ISAC-II experimental hall.